Q. J. R. Meteorol. Soc. (2002), **128**, pp. 2205–2237 doi: 10.1256/qj.01.88

Simulations of fall and early winter in the stratosphere

By G. L. MANNEY[1,2*], W. A. LAHOZ[3], J. L. SABUTIS[2], A. O'NEILL[3] and L. STEENMAN-CLARK[3]

[1]*California Institute of Technology, USA*
[2]*New Mexico Highlands University, USA*
[3]*University of Reading, UK*

(Received 25 May 2001; revised 28 January 2002)

SUMMARY

Mechanistic model simulations of fall/early winter in the northern (November and December) and southern (May and June) stratosphere are compared with observational analyses to examine the skill of the model in simulating the state of the stratosphere, including both means and variability in key fields, during six winters. While detailed success varies from year to year, the model produces a realistic climatology of and variability in the evolution of winds, geopotential heights, temperatures and wave propagation in the early-winter stratosphere. The variability and mean fields agree well with those in longer data records. The northern hemisphere (NH) simulations show a small cold bias when averaged over the 6 years, while the southern hemisphere (SH) simulations show a larger warm bias. Greater detailed success in simulations of alternate NH winters suggests the possibility of greater model skill during the westerly quasi-biennial oscillation phase, although the short record and complexity of interactions between tropics and high latitudes preclude definitive identification of such a relationship. A prominent failing of the model when using Rayleigh friction to parametrize gravity-wave drag is an inability to correctly reproduce the latitudinal structure of the stratospheric jet above about 7 hPa; this failing can be alleviated by using a non-orographic gravity-wave drag parametrization, at the expense of frequently degrading agreement of planetary-wave phases and amplitudes. The success of the model in reproducing realistic climatology and variability makes these simulations useful for more detailed studies of transport and vortex evolution in early winter.

Interhemispheric comparisons show that the early-winter circulations are qualitatively similar in the NH and SH: they are dominated by a strengthening vortex, with most wave activity being in wave 1; they both have minor warmings in a preferred location and clustered around a preferred time—early December (early June) in the NH (SH); variability in the flow shows a crescent pattern of maximum variations near 60–80° latitude centred at the location of the minor warmings (over the dateline in the NH and in the South Pacific in the SH). Interhemispheric differences are primarily in the magnitude of the variability, with a more symmetric circulation and weaker minor warmings in the SH; this is in contrast to later in the winter, when large qualitative interhemispheric differences have been seen.

KEYWORDS: Interannual variability Stratosphere–mesosphere model Stratospheric polar-vortex development

1. INTRODUCTION

While much attention has been focused on the dynamics, transport and chemistry of the polar winter stratosphere, relatively little of that has included study of the fall and early winter (late October through December in the northern hemisphere (NH), late April through June in the southern hemisphere (SH)). Baldwin and Holton (1988) and O'Neill and Pope (1990) noted from area diagnostics that there is relatively little interannual variability in the NH middle stratosphere in October and November compared with later in the winter. Although the interannual variability during this period may be small compared with that in January and February, Manney and Sabutis (2000) and Manney *et al.* (2001) showed that there is indeed considerable interannual variability during November and December in the NH, and that this variability can have important consequences for the subsequent evolution of the polar vortex and stratospheric temperatures. Manney *et al.* (2001), in particular, indicated that early-winter minor warmings may have a profound impact on the development of the vortex and low-temperature

* Corresponding author: Department of Natural Resources Management, New Mexico Highlands University, Las Vegas, NM 87701, USA. e-mail: manney@mls.jpl.nasa.gov

© Royal Meteorological Society, 2002.

region in the lower stratosphere. Understanding the interannual variability and climatology of the early-winter stratosphere is thus a key part of improving our knowledge of polar processes such as ozone loss.

Labitzke (1977, 1982) examined interannual variability in stratospheric warmings in the NH winter, and noted the common occurrence of 'Canadian' warmings in November and December. Canadian warmings are associated with large wave-1 amplitudes and a corresponding shift of the polar vortex off the pole, a nearly barotropic vertical structure, movement of a warm pool into high latitudes, and little increase in minimum high-latitude mid-stratosphere temperatures (Labitzke 1977, 1982; Clough *et al.* 1985; Juckes and O'Neill 1988; Manney *et al.* 2001). Farrara *et al.* (1992) studied the early-winter circulation in the SH stratosphere, using analyses of observational data and mechanistic model simulations. They found significant interannual variability in the intensity and timing of wave-1 amplifications, and noted the occurrence of minor warmings similar in character to Canadian warmings. Their simulations suggest that these warmings are connected to wave-1 amplification and eastward propagation near the tropopause.

Clough *et al.* (1985), Juckes and O'Neill (1988), Rosier *et al.* (1994) and Manney *et al.* (2000, 2001) have described aspects of vortex evolution and/or transport during minor warmings in November and December. Butchart and Remsberg (1986), Baldwin and Holton (1988) and Juckes and O'Neill (1988) have shown evidence suggesting that minor warmings in early winter are associated with planetary-scale wave breaking, which is in turn associated with the strengthening along the vortex edge and weakening in midlatitudes of potential vorticity (PV) and tracer gradients that results in the formation of the 'main vortex/surf zone' structure (McIntyre and Palmer 1983; McIntyre and Palmer 1984). More generally, Harvey and Hitchman (1996) noted that the Aleutian high often begins to form in late October or early November, consistent with the observations of minor warmings during this period. Waugh and Randel (1999) also showed an overview of the climatology of the polar vortices, including the fall/early-winter period, in both hemispheres. They found that the NH vortex becomes more distorted and further shifted off the pole in October through December, whereas the SH vortex becomes more symmetric and pole-centred during the equivalent period. They also noted a climatological shift of the NH vortex centre, first eastward, then westward again, in late-November/December. This shift may be related to the occurrence of wave-1 type (e.g. Canadian) minor warmings in late November and early December (e.g. Labitzke 1982; Manney *et al.* 2001).

Mechanistic primitive-equation models have been used in several studies of the winter stratosphere (e.g. Farrara *et al.* 1992; Manney *et al.* 1994a, 1999; Mote *et al.* 1998; Scott and Haynes 1998; Scaife and James 2000, and references therein). Such models have succeeded in simulating both specific events such as sudden warmings (Manney *et al.* 1994a, 1999) and the overall evolution of the stratospheric circulation (Farrara *et al.* 1992; Mote *et al.* 1998). When successful simulations are obtained, the results are useful in studying the stratospheric circulation because they provide a complete set of fields in the stratosphere that are consistent with the full equations of motion and are not routinely available in observations, and because they allow sensitivity tests to be conducted in an attempt to isolate the causes of certain phenomena (e.g. Farrara *et al.* 1992; Manney *et al.* 1994a; Scott and Haynes 1998; Scaife and James 2000).

Here we present comparisons of mechanistic model simulations of the fall/early-winter stratosphere with meteorological analyses, for six early-winter periods in each hemisphere. These simulations included transport of long-lived trace gases, for which observations are sparse. We aim to show the degree of success of the model in simulating

both the detailed evolution of stratospheric fields in individual winters, and its success in simulating realistic interannual variability and the climatology of the early-winter stratosphere. The comparison of simulated and observed meteorological fields also allows us to elucidate some characteristics of the stratospheric flow in early winter, and to contrast these between the NH and SH.

2. Model and data description

(*a*) *The USMM simulations*

The UK Universities Global Atmospheric Modelling Project (UGAMP) Stratosphere–Mesosphere Model (USMM) (Thuburn and Brugge 1994) is a spectral, primitive-equation model of the stratosphere and mesosphere. It is a 'mechanistic' model, in that a lower boundary is prescribed near the tropopause from observations. Mote *et al.* (1998) give a brief history of the USMM. The primary configuration of the USMM used here is the same as that used by Manney *et al.* (1999) and similar to those used by Mote *et al.* (1998) and MacKenzie *et al.* (1999). This configuration has 34 isobaric levels from 89.5 to 0.01 hPa, giving a vertical resolution of $\sim$1.6 km, and a lower boundary specified at 100 hPa; the model levels are shown by MacKenzie *et al.* (1999). The truncation is T42, giving a horizontal resolution of $\sim 3^\circ$. The upper boundary of the USMM is at zero pressure, thus there is no mass flow through the upper boundary. The model has extra scale-selective diffusion in the mesosphere, which, with the short radiative time-scales there, helps to damp waves and reduce the possibility of wave reflection at the boundary.

For most of the runs shown here (referred to as 'RF' runs), gravity-wave drag is parametrized by applying a simple Rayleigh friction with an altitude-dependent damping coefficient (damping times range from 116 d at and below 50 km to 1.4 d at 80 km) to the zonal wind (Thuburn and Brugge 1994; MacKenzie *et al.* 1999). The USMM can also be run with a non-orographic gravity-wave scheme, as done by Mote *et al.* (1998). The implementation of this scheme in the UGAMP general-circulation model, and some experiments with it, are described by Norton and Thuburn (1997). Briefly, the phase speed, amplitude, direction of launch and source altitude are specified for a set of globally uniform waves, which then propagate and break using the same scheme as Palmer *et al.* (1986). Some results are shown here using this scheme, referred to as 'GW' runs. The selection of gravity-wave characteristics is problematic, since we do not have reliable quantitative information; in addition, the gravity-wave parametrization used does not allow latitudinal variability or provide any means to assess interannual or interhemispheric variability (which is expected, e.g. Rind *et al.* (1988)). For the runs shown here, we began with the values used by Norton and Thuburn (1997) (14 waves, 2 with zero phase speed, and 4 each at 10, 20 and 30 m s^{-1}, launched from 100 hPa), and adjusted the amplitudes in a few test runs using one case (the NH 1992 run) to 'tune' the model results. This is not, of course, guaranteed to effect similar improvements in other years or in the SH, or to improve aspects of the simulation that are not targeted—nevertheless, it does provide an indication of the sensitivity of model characteristics to the gravity-wave parametrization. Except where otherwise noted, the results of the RF runs are shown here.

The USMM uses a version of the MIDRAD radiation scheme (Shine 1987) with seasonally and meridionally varying upwelling fluxes of IR radiation in the 9.6 μm and 15 μm wavelength regions calculated using climatological temperatures assuming that emission at 9.6 μm originates at 700 hPa and emission at 15 μm originates at 130 hPa. A prescribed, zonal-mean climatological ozone field is used in the radiation calculations; Manney *et al.* (1994a, 1995) found little difference in radiation

calculations using MIDRAD with this climatological ozone from those using three-dimensional time-varying observed or modelled ozone for NH winters and SH early winter. As was done by Manney *et al.* (1999), the model was run with online transport of long-lived trace gases initialized with three-dimensional fields reconstructed from potential vorticity (PV)/potential temperature (θ) space mappings of Upper Atmosphere Research Satellite (UARS) long-lived trace-gas data. The USMM's online transport calculation is described by Thuburn and Brugge (1994).

As in previous USMM studies, the model was forced at 100 hPa using daily geopotential heights from the UK Met Office's stratosphere–troposphere assimilation data (Swinbank and O'Neill 1994b). The model was also initialized using Met Office three-dimensional wind and temperature fields. Met Office winds and temperatures above their top level of 0.3 hPa are extrapolated up to the top USMM level using thermal wind balance in the zonal mean.

The model was initialized for the NH runs on 25 October, and run for 70 days, through 3 January, to capture the fall/early-winter period when the polar vortex is developing. The SH runs are for the corresponding time period of 25 April through 4 July. Six years were run for each hemisphere, with runs initialized in 1992 through 1997. Scaife *et al.* (2000) show analyses suggesting that most of the interannual variability in the winter (December–February in the NH) stratosphere is captured in 7–10 years of data; we may thus hope that 6 years of simulations in each hemisphere is enough to capture a majority of the typical interannual variability in these early winter periods.

(*b*) *Analysis*

The USMM results are compared with Met Office analyses to assess the performance of the model, both on a day-to-day basis and in simulating realistic variability and climatology. For comparison of individual fields in the data and model (winds, temperatures, geopotential height, PV, etc.), the model results are interpolated to the same horizontal grid as the Met Office data, and to the 'UARS' pressure levels (six levels per decade, starting at 1000 hPa) on which the Met Office data are provided. Another diagnostic used here is the Eliassen–Palm (EP) flux (e.g. Andrews *et al.* 1987, and references therein) which provides a measure of wave propagation (Mote *et al.* (1998), for example, also described its use in comparing model simulations and analyses). The EP fluxes shown here are calculated as described by Sabutis (1997) from Met Office and USMM fields after they have been interpolated to a common grid, except that Met Office or USMM winds are used, rather than winds calculated from geopotential heights. To compare the variability and climatology between the model and data, the patterns resulting from empirical orthogonal function (EOF) analyses of the USMM runs, the Met Office analyses, and a longer record of US National Centers for Environmental Prediction (NCEP) data are analysed, 6-year averages of Met Office and USMM fields are compared, and correlation coefficients are calculated for climatological daily fields from model and analysis.

For a critical comparison of the day-to-day and week-to-week skill of the model in simulating the observations, we have calculated anomaly correlations and biases between the USMM and Met Office data, as described by Lahoz (1999); these diagnostics are commonly used in numerical weather-prediction studies (e.g. Miyakoda *et al.* 1972; Simmons 1986, and references therein). The anomaly correlation (AC) at a time t is

defined as:

$$\mathrm{AC}(t) = \frac{\sum_i w_i(\Delta F_i - \overline{\Delta F_i})(\Delta A_i - \overline{\Delta A_i})}{\sqrt{\sum_i w_i(\Delta F_i - \overline{\Delta F_i})^2 \sum_i (\Delta A_i - \overline{\Delta A_i})^2}} \tag{1}$$

(with all quantities involving F_i and A_i taken at time t) where F_i is the simulated field at grid point i, A_i the analysis (Met Office) field, w_i is the fraction of the area represented by grid point i, and the sums are over all grid points within the verifying domain. $\overline{X}$ is the spatial mean of a field X over the verifying domain, and $\Delta X = X - C$, where C is a climatological field. The climatologies used here for Met Office and USMM fields are derived from the six periods of analyses and simulations, respectively. Deque (1997) indicated that 6 years should be long enough to obtain a reasonable climatology for this purpose. We have also repeated these calculations using a climatology constructed from 21 years of NCEP data; differences in the ACs are modest, and do not substantially affect any of the results presented here. The bias at time t is given by

$$B(t) = \sum_i w_i(F_i - A_i) \tag{2}$$

where F_i and A_i are taken at time t. For the runs considered here, we are interested primarily in the polar regions; thus, the domain over which the AC and bias are calculated is from 45° latitude to the pole. Anomaly correlations and biases are calculated daily, for weekly and bi-weekly averages, and for the entire 70-day period of the simulations.

To assess the significance of the AC, we followed a procedure described by Bretherton *et al.* (1999), based on calculation of EOFs for the periods and domain used in the anomaly correlations, to estimate the spatial degrees of freedom of temperature and geopotential-height fields in the stratosphere. Such calculations, for both USMM and Met Office fields for the 6 years simulated, as well as for 19 years of NCEP data, indicate that the number of degrees of freedom for the fields we are studying is near five throughout the NH stratosphere, and three or four in the SH stratosphere. Following Bretherton *et al.* (1999) again, and using the Student's t-statistic, we estimate that an AC $\gtrsim$0.7 ($\gtrsim$0.8) is significant at the 95% confidence level in the NH (SH). While we use this to formally assess the significance of the results, we note that the failure to pass such a significance test does not preclude there being a meaningful correlation between the model and analysis fields (e.g. Nicholls 2001).

3. Simulations of individual NH early winters

Figure 1 shows anomaly correlations at 10 hPa, summarizing the behaviour of the USMM for the six NH simulations. The simulations for 1992, 1994 and 1996 are successful in that the daily ACs are significant at the 95% level during most of the simulation period, and the weekly and bi-weekly ACs are generally higher than the daily AC (indicating that fields agree more closely when small day-to-day differences are averaged out). The simulations for 1993, 1995 and 1997 are much less successful by this measure, with daily, weekly and even bi-weekly ACs often below the 95% significance level. The bias between USMM and Met Office data varies from year to year in both sign and magnitude, indicating that the model produces a vortex during this period that may be either too cold/strong or too warm/weak. The size of the bias also does not appear to be closely related to the success of the simulation as measured by the AC; 1993 and 1995 have relatively small biases through most of the simulation period, but also have low ACs indicating poor agreement in spatial structure between

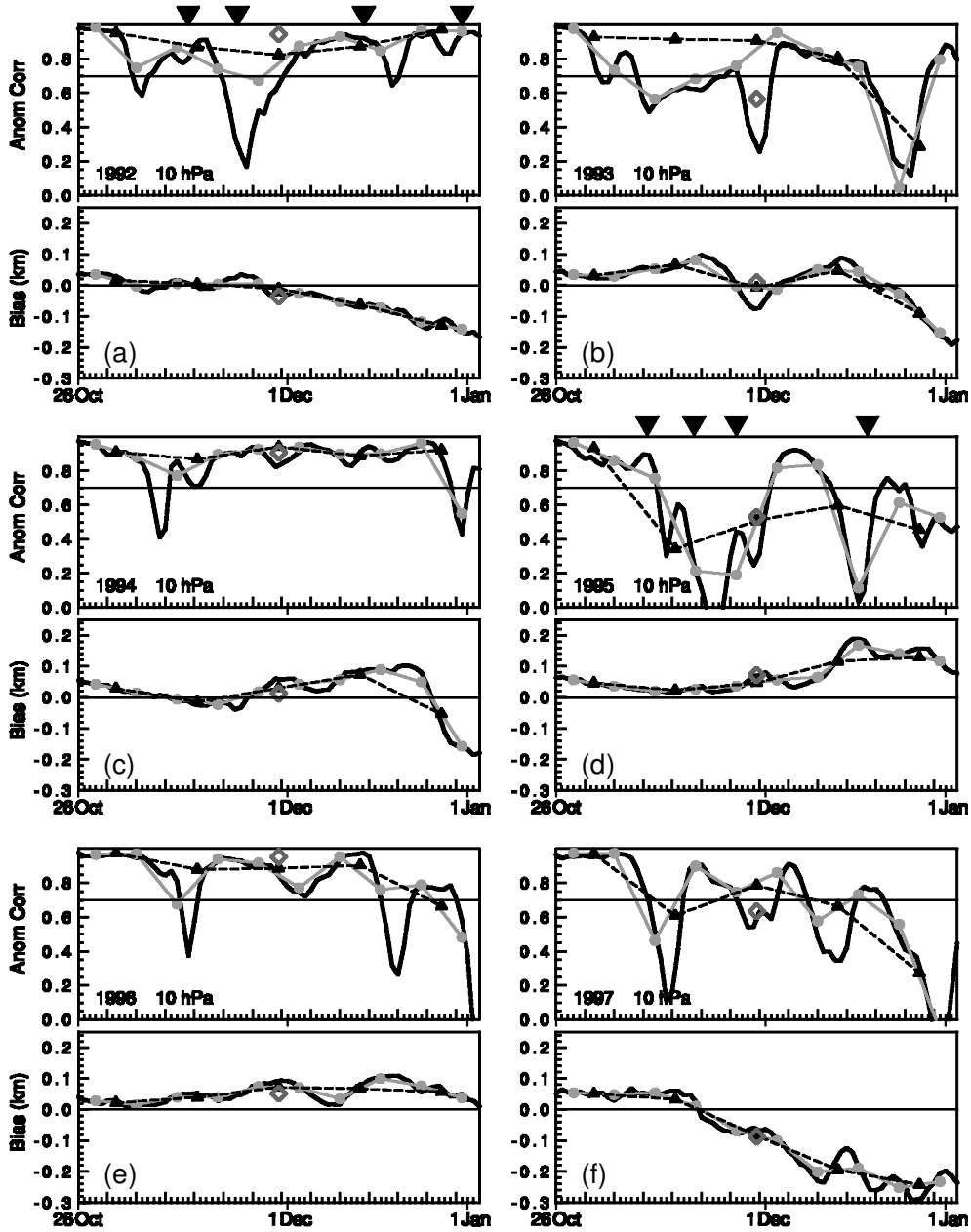

Figure 1. Anomaly correlations (upper panels, see text) and bias (km, lower panels) of 10 hPa Met Office and USMM geopotential heights for the area north of 45°N for simulations of six northern-hemisphere fall/early-winter periods. Thick black lines show correlations and biases on individual days, grey dots and lines for 7-day averages, black triangles and dashed lines, 14-day averages, and large open diamond for the average over the entire 70-day simulation period. The 95% significance level for the correlations is near 0.7 (thin horizontal line on anomaly-correlation panels, see text). Bias is calculated as USMM − Met Office, so negative values indicate lower geopotential heights in the USMM. Large black arrows at top of 1992 and 1995 plots indicate days that are shown in later figures.

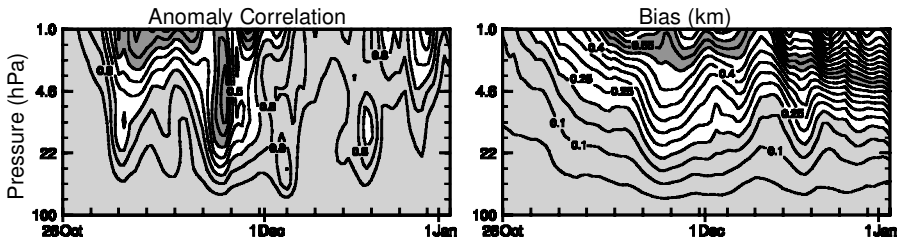

Figure 2. Anomaly correlation (AC, left) and bias (km, right) of Met Office and USMM geopotential heights for the area north of 45°N for the simulation of the 1992 fall/early winter, as a function of pressure throughout the stratosphere. AC contour interval is 0.1; values greater than 0.7 are lightly shaded, and below 0.4, darkly shaded. Bias contour interval is 0.05 km; values less than 0.2 km are lightly shaded, and values from 0.5 to 0.6 km darkly shaded.

the model and Met Office analyses. Figure 2 shows the daily AC and bias for the 1992 simulation as a function of altitude. These are typical of other simulations as well, in that the agreement is better at lower levels and worse at higher levels. Better agreement is expected, AC approaching one, as the model lower boundary (100 hPa) is approached. While agreement becomes worse in the upper stratosphere, for successful simulations such as this one, the AC remains above the 95% significance level during most of the simulation period.

In the following, we will examine in detail some of the model fields that result in these correlations, for successful and unsuccessful simulations. We concentrate on the simulations for 1992 (along with 1994 the most successful simulation) and 1995 (the least successful). To ensure that the exact initialization date does not have a strong influence on the success of the simulations, we analysed simulations started 4 days earlier and 4 days later for these two years. The results from all of these runs were very similar to those shown in Fig. 1 with, e.g. dips in the AC at approximately the same times and to approximately the same values.

The time evolution of the 10 hPa zonal-mean wind and temperature, and wave-1 and wave-2 geopotential-height eddies in 1992 and 1995 is shown in Fig. 3; Fig. 4 shows USMM–Met Office differences in zonal-mean wind and temperature for those years. Figure 4 shows larger and more persistent differences in zonal-mean wind throughout the simulation in 1995 than in 1992, with a dipole pattern of differences indicating that the model jet is centred at higher latitudes than that in the Met Office analyses. Temperature differences are of the same magnitude in both years, but more persistent throughout the simulation in 1995. The most dramatic difference between the zonal means occurs in late December 1995, when the USMM produces a minor warming that is much stronger than that seen in the Met Office data. In both years, the USMM somewhat underestimates polar temperatures through much of the simulations. The combined wave-1 and wave-2 amplitudes in the USMM are quite similar to those in the Met Office analyses in both years, but the relative amplitudes of wave 1 and wave 2 shows some differences between model and analysis (Fig. 3). In 1992, the phases of both wave 1 and wave 2 show good agreement between Met Office and USMM throughout the simulation; in 1995, on the other hand, both wave-1 and wave-2 phases show significant differences beginning in late November. This suggests that part of the larger difference in spatial structure in 1995, as indicated by the anomaly correlations, results from discrepancies in the longitudinal position of the vortex.

Figure 5 shows NH 10 hPa geopotential-height maps for the 1992 and 1995 periods, on the days marked by arrowheads in Fig. 1, chosen to illustrate times of good and poor

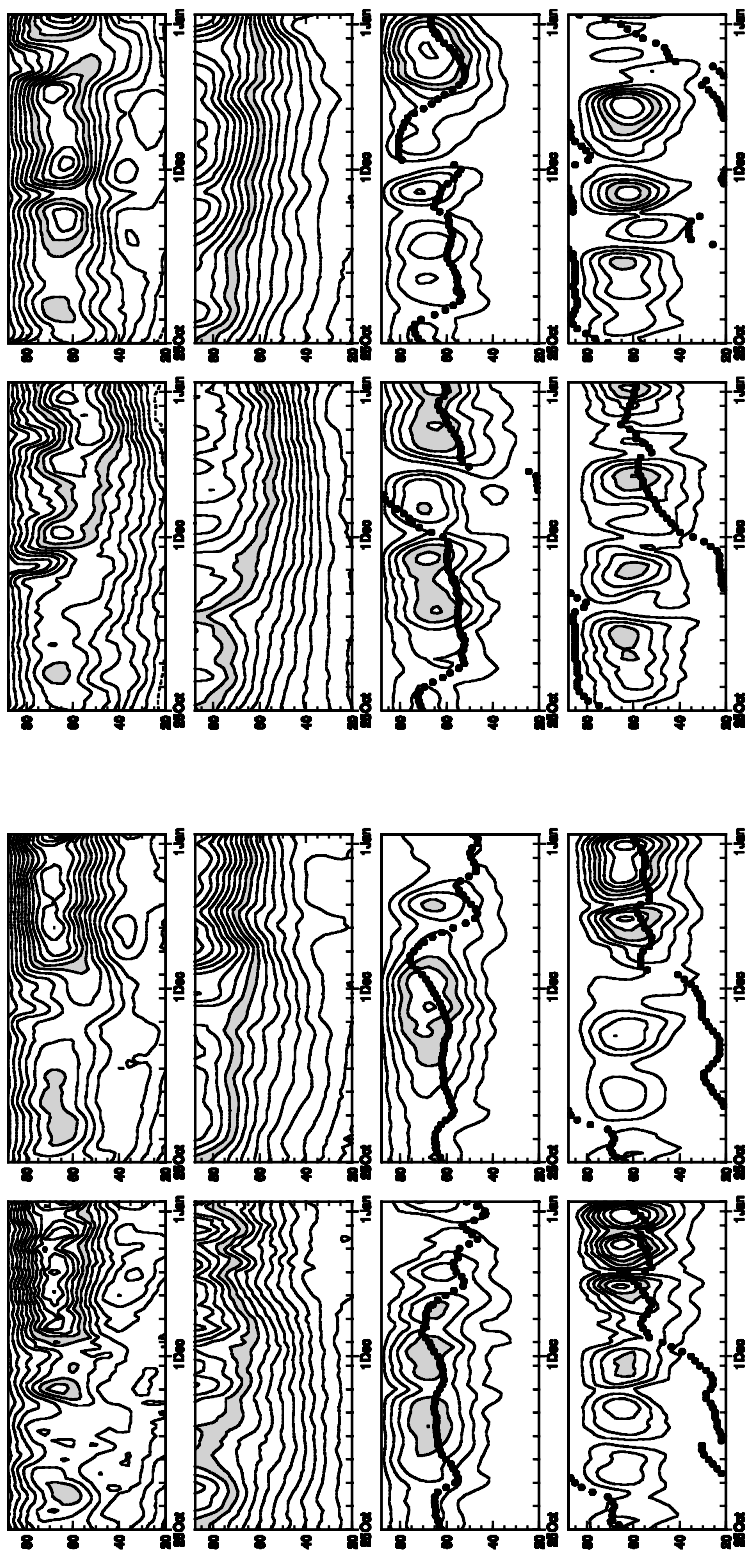

Figure 3. Time series for 25 October through 3 January of (top to bottom) zonal-mean wind, zonal-mean temperature, geopotential-height wave 1 and geopotential-height wave 2 at 10 hPa in the northern hemisphere, from (left two columns) Met Office and USMM in 1992, and (right two columns) Met Office and USMM in 1995. Zonal-wind contour interval is 5 m s^{-1}, with 30–35 m s^{-1} shaded; temperature contour interval is 2.5 K, with 207.5–210 K shaded; wave-1 contour interval is 0.2 km, with 0.8–1.0 km shaded; wave-2 contour interval is 0.1 km, with 0.4–0.5 km shaded. Black dots on wave-1 and wave-2 plots show phase (longitude of one maximum) from 0 (bottom) to 360°E (top).

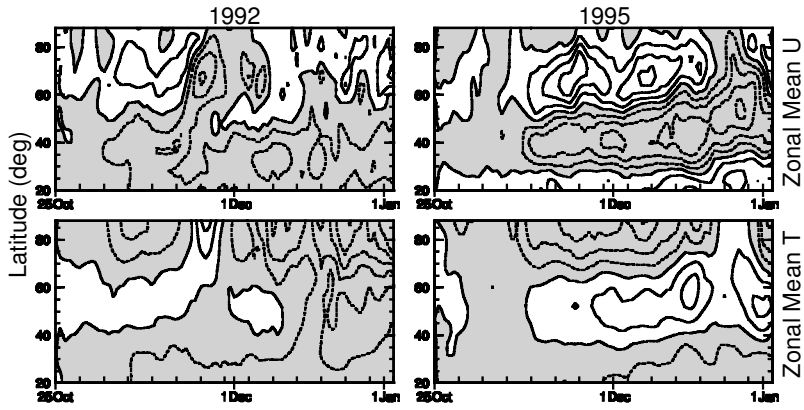

Figure 4. USMM–Met Office differences in 10 hPa zonal-mean winds (top) and temperature (bottom) for 1992 (left) and 1995 (right). Wind contour interval is 5 m s^{-1}; temperature interval is 3 K. Differences less than zero are shaded.

agreement between model and analysis. Good overall agreement is seen in all the maps shown for 1992. The first two maps for 1992 are from the two times when the AC dips slightly below the 95% significance level, and show (especially for 21 November) small but distinct differences in the shape and position of the vortex and the depth of the anticyclone. Agreement in shape and position of vortex and anticyclone appears very good on the latter two days shown, when the AC was high (0.85 to 0.9). A somewhat different picture is seen for 1995. On 9 November, the AC was high (Fig. 1), and the shape and position of vortex and anticyclone agree well between model and analysis. The other 3 days shown are during periods of very low AC. Most of the difference between USMM and Met Office maps on 24 November and 19 December is in the positions of the vortex and anticyclone, with the model fields being shifted $\sim 15^\circ$ west on 24 November and $\sim 30^\circ$ east on 19 December. The differences between USMM and Met Office on 19 November are more dramatic. At this time, both wave 1 and wave 2 in the model are slightly smaller than in the Met Office analysis, and the USMM wave-2 phase is shifted nearly 90° east from that in the Met Office (Fig. 3). The wave-2 phase shift accounts for a large part of the apparent difference between the two fields. Overall, the agreement of individual daily maps for 1995 between the USMM and Met Office fields is not as poor as suggested by the AC in Fig. 1, in that for most of the period, the low AC values arise primarily from relatively small differences in the position of the vortex (e.g. 24 November and 19 December). This underscores the sensitivity of pattern correlations to small differences, which makes them a very stringent measure of agreement.

Figure 6 shows the 32 hPa EP flux divergence as a function of time. In 1992, the Met Office and USMM divergences agree, in that there are generally similar regions of convergence and divergence at approximately the same time and with a similar latitudinal extent. The only time when this is not the case is around 20 November, when the Met Office field shows a region of divergence (acceleration of the jet) at high latitudes that does not appear in the model field. This is also one of the times when the AC between model and analysis was lower. Toward the end of the 1992 period, the model shows weaker regions of divergence and, especially, convergence than the Met Office analysis, but with the correct timing and locations. This is consistent with the increasing cold bias of the model at the end of this run (e.g. Fig. 1). In 1995, more

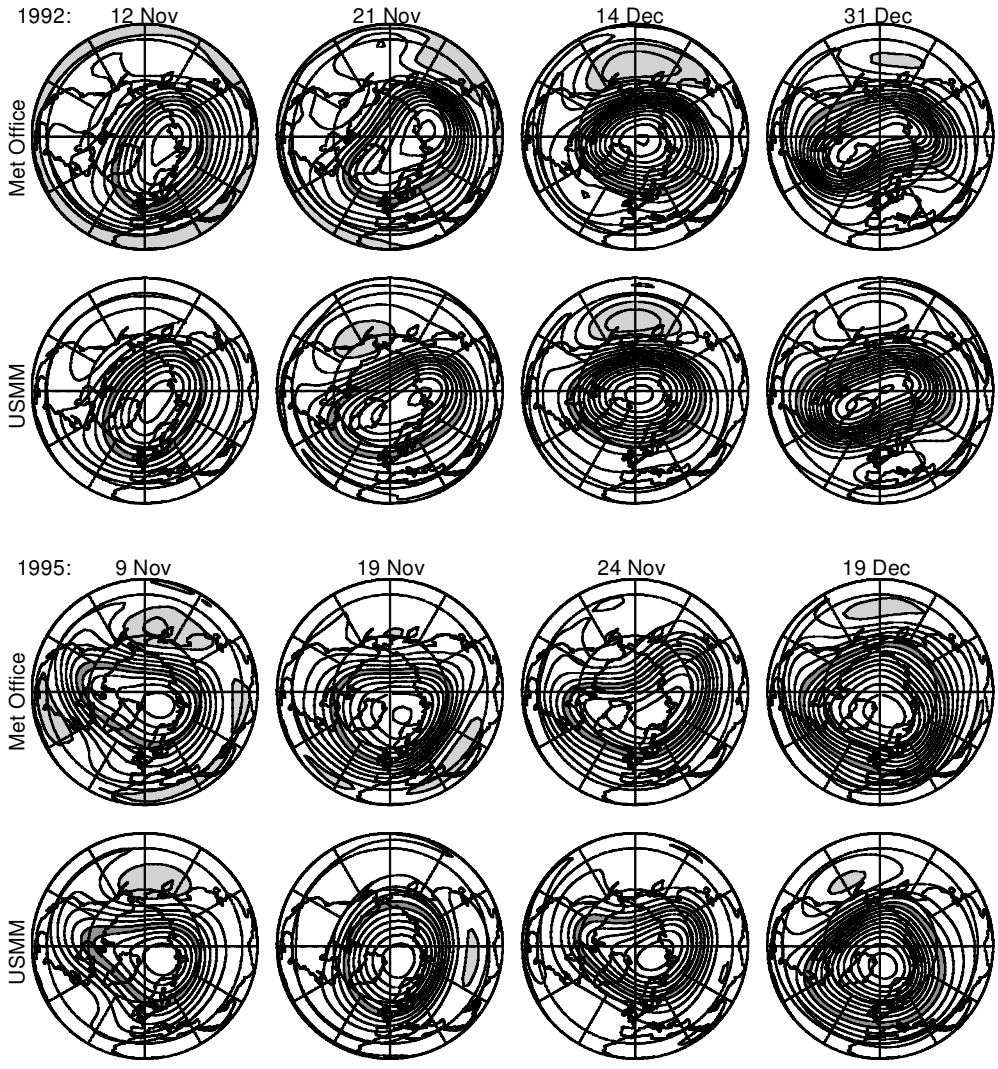

Figure 5. Maps of 10 hPa geopotential height on selected days during the simulations of the 1992 (top two rows) and 1995 (bottom two rows) early northern-hemisphere winters; for each year, the upper row shows Met Office and the lower row USMM fields. Contour interval is 0.2 km, with dark shading from 29.8 to 30 km and light shading above 31 km. Projection is orthographic, with 0° longitude at the bottom, and 90°E to the right. Domain is from equator to pole with dashed circles at 30 and 60°N.

qualitative differences are seen between the model and analysis, but for much of the period they still show similar patterns. In the 15–25 November period, the Met Office field shows weak regions of convergence which do not appear in the USMM simulation, although it might be argued that the latter of these (near 50–60°N on ~20–23 November) might simply be appearing a few days earlier than the region of convergence in the USMM. In the second half of the run, the differences are more quantitative than qualitative, with the Met Office fields showing much stronger convergence (deceleration of the jet) in early December than the model produces. Near mid-December, the region of strong convergence appears 2–3 days earlier in the USMM than in the Met Office analysis. Figure 7 compares model and Met Office 60°N EP flux divergences at 32,

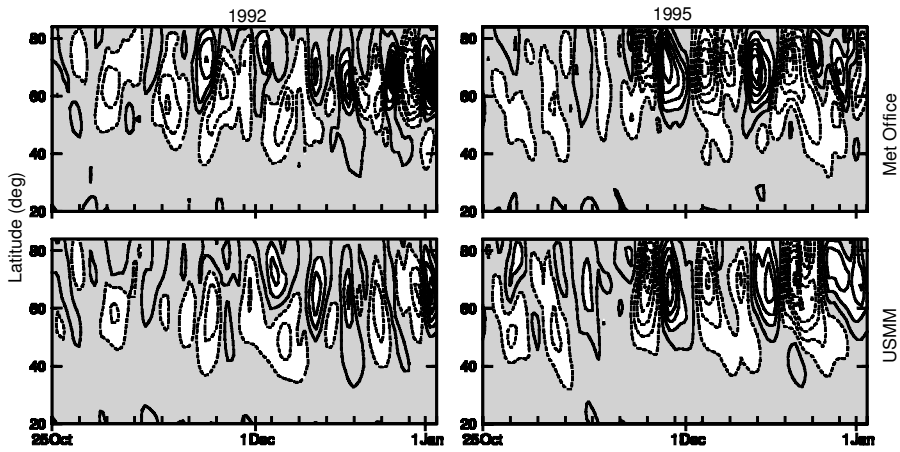

Figure 6. Eliassen–Palm flux divergences (m $s^{-1}d^{-1}$) as a function of time and latitude at 32 hPa, for 1992 (left) and 1995 (right), from Met Office (top) and USMM (bottom). Contour interval is 2 m $s^{-1}d^{-1}$, with values from −2 to 2 m $s^{-1}d^{-1}$ shaded, and dashed lines for negative values.

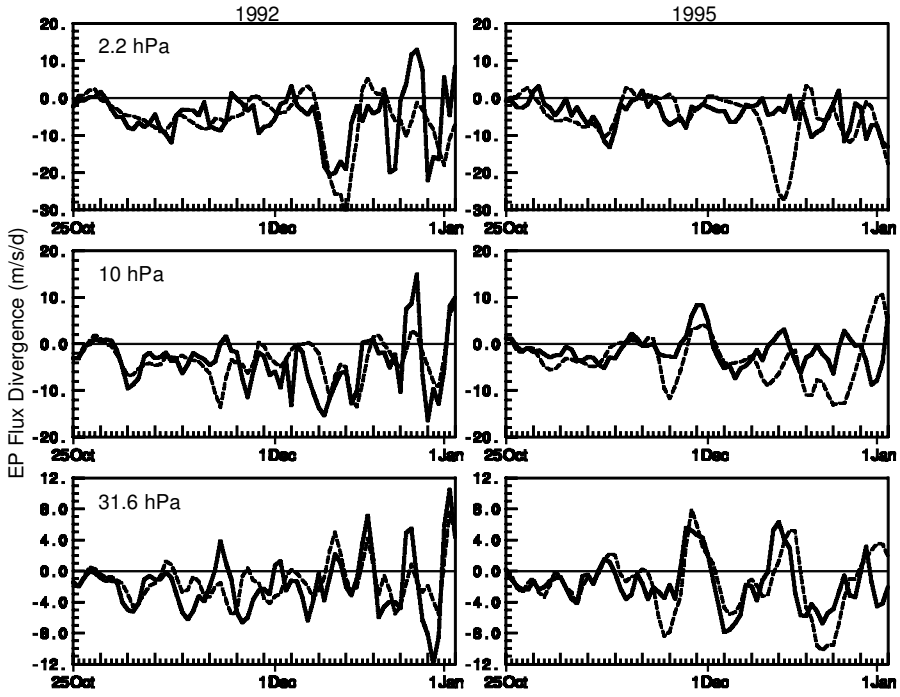

Figure 7. Eliassen–Palm flux divergences (m $s^{-1}d^{-1}$) at 60°N as a function of time, for 1992 (left) and 1995 (right), at 2.2 (top), 10 (centre) and 32 hPa (bottom). Solid lines show Met Office and dashed lines USMM results. Note that there are different divergence ranges at different levels.

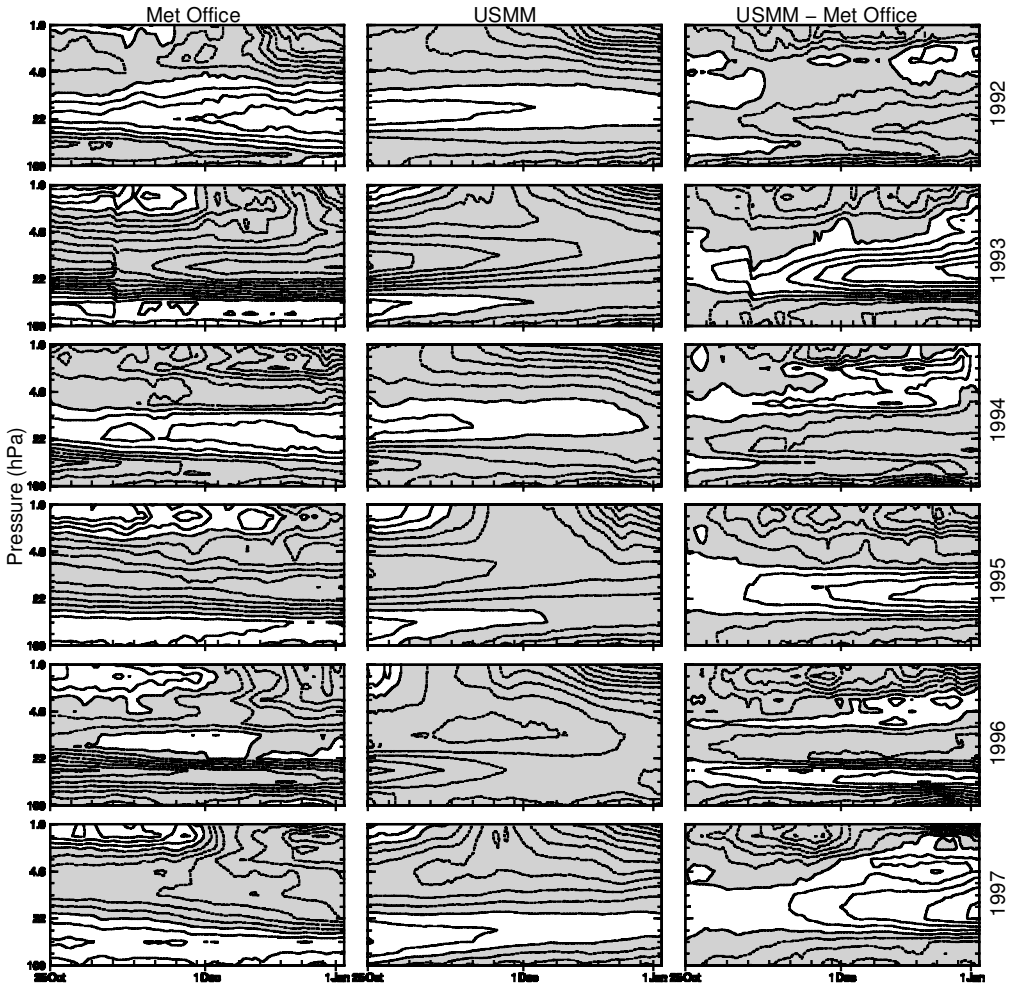

Figure 8. Zonal-mean equatorial winds (m s^{-1}) for the periods of the six northern-hemisphere simulations, from Met Office (left), USMM (centre) and the difference, USMM – Met Office (right). Contour interval is 4 m s^{-1}; values less than zero are shaded.

10 and 2.2 hPa, showing fairly good agreement at all levels through most of the 1992 period. The 1995 case shows a few periods of poor qualitative agreement (e.g. late November and late December at 10 hPa, mid-December at 2.2 hPa), but also many times where disagreement is due only to small differences in timing or magnitude (e.g. mid-December at 32 hPa). The two-dimensional (2D) EP fluxes shown here average out the instantaneous planetary-wave phase information, and may thus show good agreement even when the phases of planetary waves disagree. Preliminary examination of 'three-dimensional EP fluxes' (e.g. Plumb 1985; Sabutis *et al.* 1997) suggests that there are significant differences in the local (three-dimensional) patterns of planetary-wave propagation between the model and Met Office analyses in the poorer simulations.

Although 6 years is too short a time to conclusively detect a pattern, the greater success of the model in even years than in odd years does raise the question of whether the phase of the quasi-biennial oscillation (QBO) may play a role in model skill. Figure 8

shows equatorial zonal-mean winds as a function of pressure during each of the simulations, and the difference between USMM and Met Office winds. The Met Office analyses contain a realistic representation of the QBO (e.g. Swinbank and O'Neill 1994a; Randel *et al.* 1999). In 1992 and 1994, Fig. 8 shows steady or increasing westerlies in the NH tropical stratosphere between ~30 and 10 hPa; in 1993 and 1995, there were steady or increasing easterlies in this altitude region. In 1996 there were weak westerlies in the mid-stratosphere (20–10 hPa), and in 1997, descending and increasing easterlies above ~20 hPa. The polar-vortex strength does not very closely follow the paradigm of weaker polar vortices during easterly QBO years (e.g. Baldwin *et al.* 2001, and references therein), as the early-winter polar vortex was unusually strong in December 1993, 1994, and 1995 (strongest in 1994) (Manney *et al.* 1994b, 1996; Zurek *et al.* 1996), and unusually weak in 1996 (e.g. Coy *et al.* 1997) (the definition of QBO phase in November and December 1996 would depend on the altitude used to define it). Because the tropical waves that are thought to force the QBO (some combination of Kelvin, Rossby-gravity, inertia-gravity and gravity waves, e.g. Baldwin *et al.* (2001), and references therein) are largely not represented in the USMM (due to inadequate resolution and/or the forcing for the equatorial lower boundary not producing significant vertical momentum flux associated with these waves), the USMM equatorial winds tend to relax toward low values (presumably toward zero or weak easterlies in the lower to middle stratosphere, although the relaxation is not fast enough to see that in these 70-day runs). This relaxation is faster when winds are stronger, so low-latitude model–analysis differences are largest in 1993 and 1997 (Fig. 8). However, the years with poorer Arctic simulations do not show obviously 'worse' performance in the simulation of the QBO itself (e.g. 1992 and 1995 equatorial USMM winds depart from analysed winds at about the same rate). Detailed examination of 2D EP fluxes, including at middle and low latitudes (where Dunkerton and Baldwin (1991) noted differences in planetary-wave fluxes between easterly and westerly QBO phases) also does not indicate a consistent pattern of model–analysis differences in years with poor versus good simulations.

Equatorial winds in the GW runs (using the non-orographic gravity-wave parametrization rather than the Rayleigh friction, described in section 2(a)) depart much more slowly (in each year) from the analysed winds than those from the RF runs shown here; this is perhaps not surprising, since it has been shown that a QBO can be produced and maintained in a mechanistic model solely by adding a non-orographic gravity-wave parametrization (Lawrence 2001). However, the GW runs have lower, rather than higher, ACs for the poor simulations in 1993, 1995 and 1997. Examination of synoptic fields indicates that the degradation results mainly from larger planetary-wave phase differences between model and analysis, and also at some times from larger planetary-wave amplitudes in the GW runs. The lack of improvement in easterly QBO years in the GW runs suggests that, if there is a dependence of model skill on the QBO phase, it may not be directly related to how well or how poorly the model simulates the QBO.

As shown above, model–analysis differences in the Arctic are dominated by planetary-wave phase differences, and also some differences in wave-1 and wave-2 relative amplitudes; in addition, as seen in Fig. 8 for the equatorial winds, the model–analysis differences for synoptic or zonal-mean fields and diagnostics do not show obviously different patterns between good and poor simulations. The complexity of the interactions between low-latitude zonal-mean winds, the gravity-wave parametrization, and planetary-wave propagation and evolution, and the few QBO cycles represented in just 6 years of simulations, make it difficult to deduce whether the QBO may be a significant factor in determining the quality of the simulations.

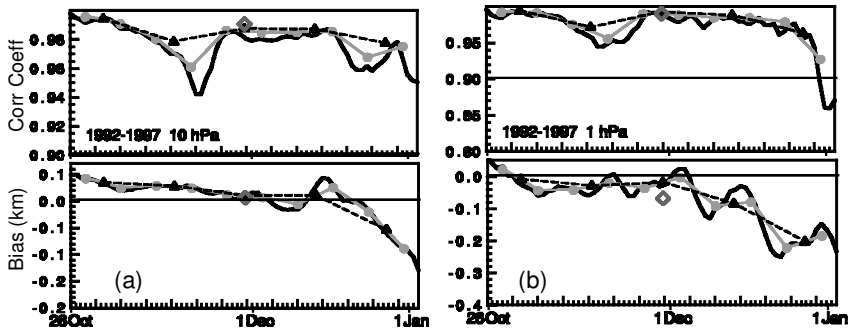

Figure 9. Correlation coefficients (top panels) and bias (bottom panels) between 'climatological' (i.e. 6-year average) Met Office and USMM daily geopotential-height fields at (left) 10 hPa and (right) 1 hPa, for the area north of 45°N. Bias is calculated as USMM − Met Office, so negative values indicate lower geopotential heights in the USMM. The 0.9 correlation-coefficient line is shown for reference on the 1 hPa anomaly-correlation plot. Lines and symbols are as in Fig. 1.

Much more detailed study, including simulations of many more early-winter periods, and perhaps model runs with an imposed QBO (similar to those done by Gray (2000) and Gray *et al.* (2001)) would be needed to determine the possible role of the QBO in the skill of the simulations.

Although the anomaly correlations shown in Fig. 1 indicated poor agreement between the USMM simulations and Met Office analyses in 3 of the 6 years, examination of the daily fields in fact shows fair agreement between many model and analysis characteristics. While the somewhat limited success of some USMM simulations of NH fall and early winter may preclude using these simulations for detailed studies of those particular periods, this suite of simulations may still prove useful in studying stratospheric variability during early winter. In the next section we examine the question: how realistically does the USMM simulate the climatology and variability in these six NH early-winter periods?

4. Overview of simulated climatology and variability in the NH

Figure 9 shows the correlation coefficient and bias between daily climatologies (i.e. point-by-point averages of the fields on the same day in the six different years) constructed from the Met Office and USMM geopotential-height fields at 10 and 1 hPa, for the area north of 45°N (note that the lower end of the correlation-coefficient axis is 0.9 at 10 hPa and 0.8 at 1 hPa). The correlations indicate a very strong similarity between the average development of the polar vortex in the model and analyses. At both levels, there are minima in the correlations in late November and late December, consistent with the time periods in Fig. 1 when anomaly correlations are lower in several years. Despite the variability in biases for individual years, overall the model produces geopotential heights that are too low (i.e. the model vortex is too strong/cold) toward the end of the simulations.

Figure 10 shows 6-year average time series of 10 hPa zonal-mean wind and temperature, and wave-1 and wave-2 geopotential height, from the model and Met Office analyses, and the differences between them. Consistent with the model bias seen in Fig. 9, the USMM results show slightly stronger winds, lower temperatures, and smaller wave-1 amplitudes in mid to late December; as was the case for individual years, the wind differences show a dipole pattern indicating that the model jet tends

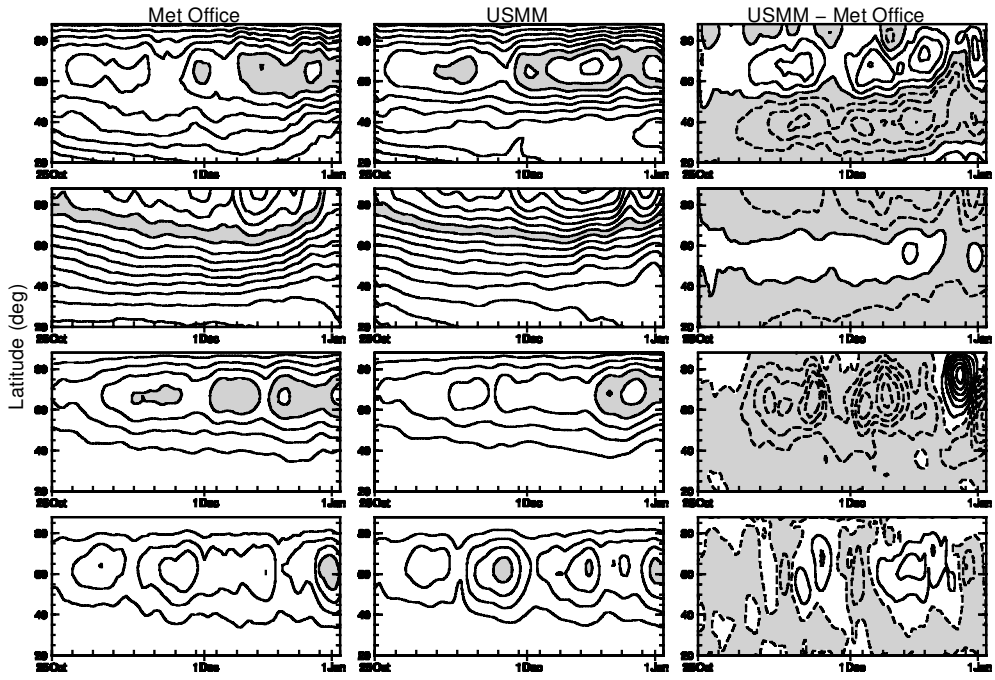

Figure 10. Time series of 6-year average (top to bottom) zonal-mean wind, zonal-mean temperature, geopotential-height wave 1 and geopotential-height wave 2 at 10 hPa in the northern hemisphere, from Met Office (left), USMM (centre) and the difference (USMM – Met Office, right). Contour intervals and shading for Met Office and USMM fields are as in Fig. 3. Contour intervals for difference plots are 3 m s^{-1}, 3 K, and 0.05 km for wind, temperature and geopotential height, respectively; negative difference values are shaded.

to peak at higher latitude. The time evolution of all fields is qualitatively similar in the model and analysis. Zonal-mean winds show a decrease in late November, concurrent with an increase in wave amplitudes, indicating a preferred time for early-winter minor warmings. The increase in wave 2, as well as wave-1, amplitude at this time suggests that the warmings do not always closely follow the Canadian warming pattern. A slightly larger amplification of wave 2 and smaller amplification of wave 1 in the model point to differences in wave activity being partially responsible for the reduced correlation between model and analysis seen in Fig. 9. The analysis in the previous section showed that, for individual years, poorer agreement during this time period is also related to phase differences between USMM and Met Office waves. Overall, Fig. 10 shows good agreement between the general features of vortex development and evolution in the USMM simulations and the Met Office analyses.

An overview of the vertical structure of USMM and Met Office climatological wind and temperature fields is given in Fig. 11(a), showing wind speeds and temperatures as a function of equivalent latitude (the latitude that would enclose the same area as a given PV contour, e.g. Butchart and Remsberg (1986)) and θ averaged over the 6 years and over 5-day periods throughout the simulations. This gives a vortex-centred view of the strength of the winds and vortex, and, in the position of maximum wind speeds, the size of the vortex (Manney and Sabutis 2000). Modelled upper-stratospheric winds are too strong in the 30 December–3 January period, but agreement is good in each period below ~840 K. The most obvious model–analysis differences are the model's failure to capture the strength of the equatorward leg of the upper-stratospheric double

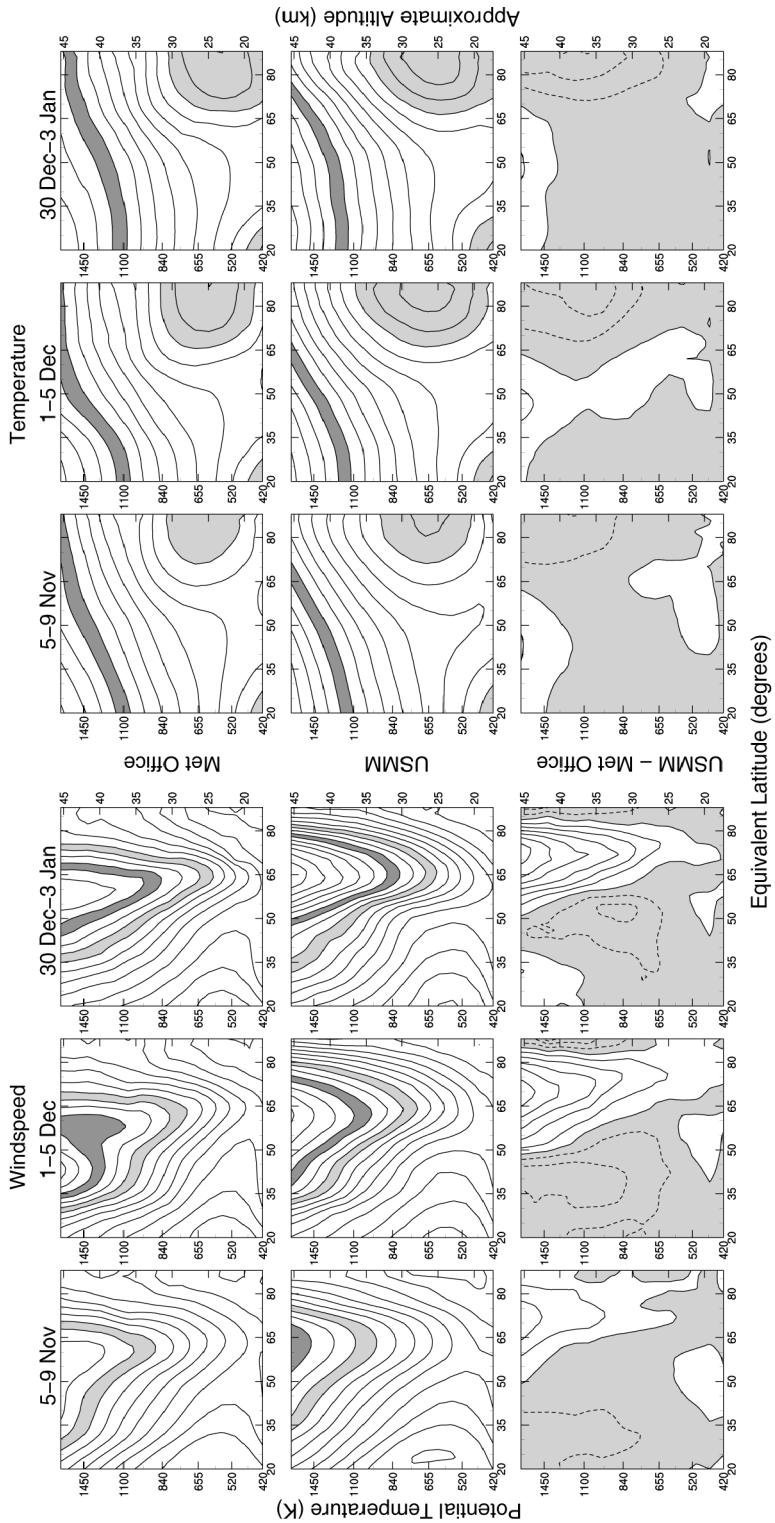

Figure 11. (a) Cross-sections of wind speed (left columns) and temperature (right columns) as a function of θ and equivalent latitude averaged over 5-day periods and over the 6 years simulated in the northern hemisphere, for Met Office (top), USMM (centre, RF runs, see text) and the difference, USMM – Met Office (bottom). Wind-speed contour interval is 5 m s^{-1}, with 45–50 m s^{-1} lightly shaded and 60–65 m s^{-1} heavily shaded; temperature contour interval is 5 K, with light shading below 205 K and heavy shading from 240 to 245 K. Contour intervals for difference plots are 5 m s^{-1} for winds and 5 K for temperatures, with negative values shaded. (b) Cross-sections of wind speed (top two rows) and temperature (bottom two rows) as a function of θ and equivalent latitude for the same periods as in Fig. 11(a), for USMM runs with the non-orographic gravity-wave parametrization (GW runs), from the USMM, and USMM–Met Office differences. Contours and shading are as in Fig. 11(a).

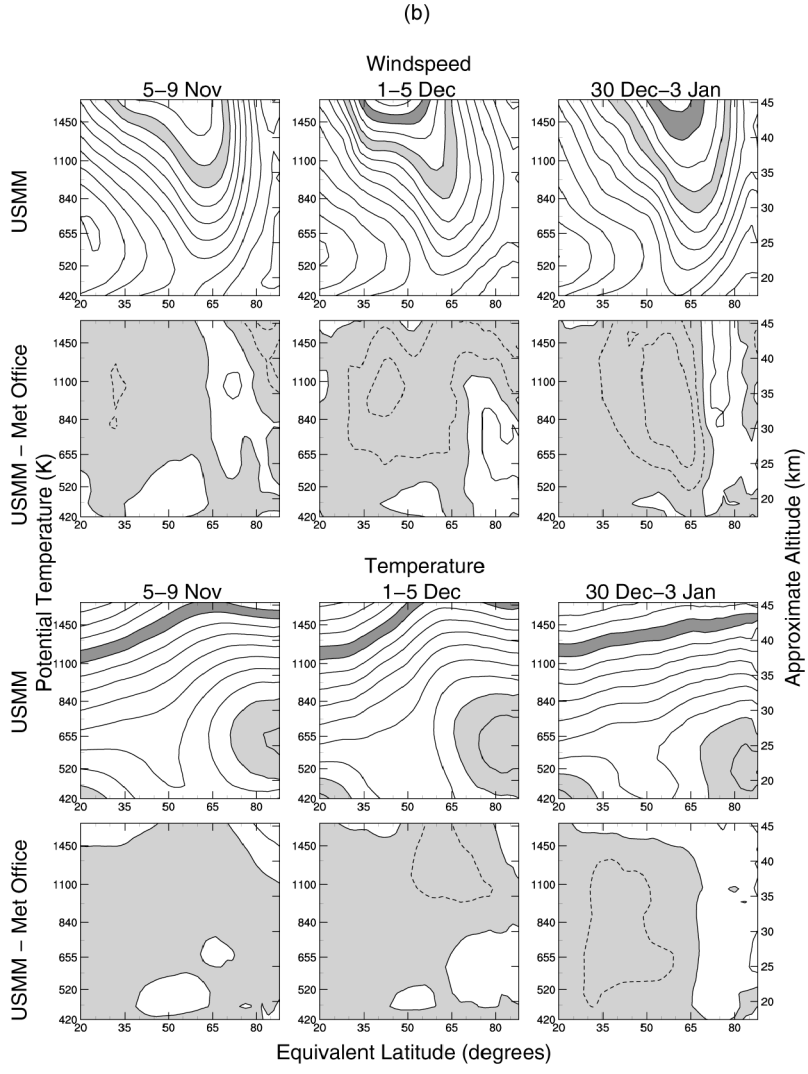

Figure 11. Continued.

jet in the 1–5 December period, and the poleward shift of the model jet with respect to that in the Met Office analyses in December. The double jet is a common, but not ubiquitous, feature of the upper-stratospheric flow in November to December (Manney and Sabutis 2000). Examination of the individual simulations shows that even in years with otherwise good simulations (e.g. 1992 and 1994) the model does not reproduce the strength of the equatorward branch of the upper-stratospheric double jet. Swinbank *et al.* (1998) reported simulation of an upright rather than equatorward-tilted polar-night jet in a general-circulation model using a similar Rayleigh-friction parametrization of gravity waves. Consistent with this, the failure of the USMM to reproduce the detailed structure of the upper-stratospheric zonal wind is largely related to this simple parametrization of gravity-wave drag; Fig. 11(b) shows USMM and difference plots of the same fields from the GW runs; the shape and strength of the jet in the upper stratosphere are much closer

to those in the Met Office analyses, although the poleward shift of the USMM jet in the middle stratosphere remains. Another possible factor in the reduction in skill in the upper stratosphere is the model initialization for winds and temperature assumed above 0.3 hPa (section 2(a)), although it is hoped that this would not be a large effect because of the fast radiative times-scales at these levels; it is difficult to test this initialization scheme, since meteorological analyses for initializations that extend above 0.3 hPa are not generally available.

Overall, temperatures in the RF USMM runs (Fig. 11(a)) are too low in the vortex centre throughout the stratosphere, leading to stronger equator-to-pole temperature gradients, consistent with the stronger vortex in the model simulations. The GW runs give polar temperatures that are slightly high in the lower stratosphere. Although the GW runs' wind and temperature climatologies are overall closer to those in the Met Office analyses than those from the RF runs, examination of synoptic fields and time evolution in the middle and lower stratosphere shows larger planetary-wave phase and amplitude differences in many of the GW simulations, and often larger zonal-mean wind differences in the middle stratosphere. Thus, the GW runs cannot be considered universally more successful than the RF runs, although they may be more useful for some studies. The qualitative patterns in the temperature fields and their time evolution are very similar in the model and Met Office analyses (Fig. 11).

To examine in more detail the structure and evolution of the NH early-winter stratosphere and interannual variability therein, in Fig. 12 we present time means and standard deviations of the 10 hPa geopotential-height fields for the entire simulation period, and the first three principal components (PCs) of the variability in the 10 hPa geopotential height from EOF analyses, for the 6 years simulated in both USMM and Met Office analyses and, for comparison with a longer time record, for 19 years of NCEP data for the same fall/early-winter time period. EOFs calculated from the anomaly fields (model or analysis minus climatology) provide a similar picture. The time means in all three cases show a nearly identical shape of the polar vortex, with a slightly deeper vortex in the USMM than in either the Met Office or NCEP analyses. In each case, the standard deviations show maximum variability near 60–80°N in a crescent centred just east of the dateline. This is the region where the Aleutian high is forming. Not only does the timing of formation and intensity of the Aleutian high vary from year to year, but also early-winter minor warmings (often of the Canadian warming type) typically result in temporary intensification, and sometimes longitudinal displacement, of the developing Aleutian high (e.g. Harvey and Hitchman 1996). The standard deviations shown here indicate that it is the variability (both interannual and intraseasonal) associated with these processes that is dominant in the NH fall and early winter. Examination of standard deviations from averages over the 6 years (interannual variability) for periods throughout the runs, and standard deviations for averages over each individual run (intraseasonal variability) show that the maximum in interannual variability is in a similar position throughout the early-winter period. The intraseasonal variability, however, maximizes in different regions each year, although there is usually a region of strong variability in the 90–270°E hemisphere. The variability shown in Fig. 12 thus reflects predominantly the patterns of interannual variability. In contrast to the pattern of interannual variability seen here, Scaife *et al.* (2000) found that interannual variability in NH mid-to-late winter (January/February) maximized over the pole in a nearly zonally symmetric pattern. The general agreement in magnitude and position of the standard deviations between USMM, Met Office and NCEP indicates that (1) the model produces a realistic pattern of interannual and intraseasonal variability, and (2) the variability in the 6-year period of the Met Office analyses and USMM simulations is generally representative of that

Figure 12. Time mean, standard deviation and first three empirical orthogonal functions of the 10 hPa geopotential heights in the northern hemisphere for 26 October through 3 January from (top) USMM for 6 years, 1992–97; (centre) Met Office for 6 years, 1992–97; and (bottom) NCEP for 19 years, 1979–97. Geopotential-height contour interval is 0.2 km, with 29.8–30 km shaded; standard-deviation contour interval is 0.04 km, with 0.52–0.56 km shaded. Principal component (PC) fields are normalized, with contours from −1 to 1 by 0.1 and negative values shaded. Note that PC#3 in the USMM is a pattern corresponding to PC#2 in the Met Office and NCEP analyses (see text).

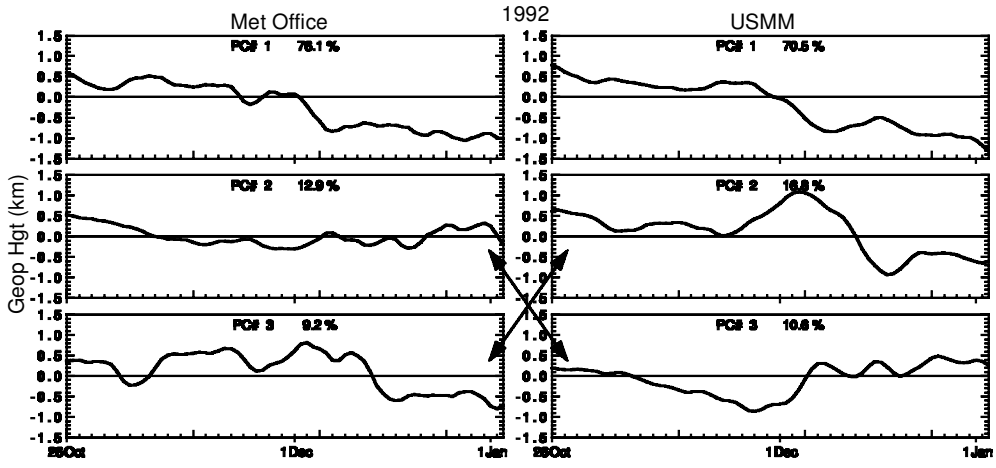

Figure 13. Time projections of 10 hPa geopotential height onto the first three empirical orthogonal functions from (left) Met Office and (right) USMM, for the 1992 northern-hemisphere early winter. Note that PC#3 in the USMM is a pattern corresponding to PC#2 in the Met Office analysis (see text).

in the longer-term record (although most of the differences between the Met Office and NCEP patterns seen in Fig. 12 are due to the longer NCEP record—patterns from NCEP for the same 6 years are very close to those from the Met Office analyses). That 6 years gives a fair representation of the interannual variability is perhaps not unexpected, as Scaife *et al.* (2000) noted that 7–10 years (depending on altitude and month) was long enough to capture 95% of the variability in winter (December, January and February in the NH).

In each of the three EOF analyses, the first three PCs (which explain ~98% of the variance) are very similar, and comprise an annular mode and two patterns dominated by wave 1 approximately 90° apart in phase. While PC#2 and PC#3 are very similar in the Met Office analysis and the longer time record of NCEP analysis, PC#3 (#2) in the USMM corresponds approximately to PC#2 (#3) in the analyses. This underscores the strong role of model–analysis phase differences in many disagreements between the USMM and Met Office. The similarity between the PCs for the three EOF analyses again indicates realistic representation of the typical patterns of variability in early winter in the model, although the dominance of a phase-shifted pattern (i.e. PC#2 in the USMM corresponding to PC#3 in the analyses) in the USMM reflects a persistent phase difference between model and analysis. EOFs for the GW runs in the NH show similar PC#1 (70%) patterns, a stronger PC#2 (19%) pattern, and a PC#3 (6%) pattern phase shifted ~30° west from that in the RF runs; PC#4 (not shown) explains ~4% of the variance in the GW case, as opposed to less than 1% in the RF runs and the analyses.

An example of the time projection of the 10 hPa geopotential heights on the Met Office and USMM PCs is shown in Fig. 13. While there is considerable interannual variability in these time projections in the NH, this example is representative of the overall vortex evolution and how it compares between the USMM and Met Office analyses. The decreasing trend in the projection on PC#1 throughout the period to substantial negative values is indicative of the strengthening of the polar vortex with time. Comparing the evolution of the projection on Met Office PC#2 with that for USMM PC#3, and Met Office PC#3 with USMM PC#2, shows generally similar evolution of these wave-1-dominated patterns; the correlation coefficients for PC#1,

Met Office PC#2 with USMM PC#3, and Met Office PC#3 with USMM PC#2 are 0.96, 0.63 and 0.88, respectively; that for Met Office PC#3 with USMM PC#2 is significant at the 99% confidence level (the degrees of freedom for each series are estimated using a measure of the autoregressive property (Livezey and Chen 1983) and are used to calculate a confidence level (Freund 1971)); for PC#1, the degrees of freedom are too few to estimate a confidence level. A similar level of agreement is seen in other years, even those such as 1995 when detailed agreement between model and analyses is not as good, with correlation coefficients usually significant at or near the 95% level. Exceptions are Met Office PC#3 with USMM PC#2 in 1993 (when there were large phase differences in both wave 1 and wave 2 between USMM and Met Office) and PC#1 in 1997 (when a strong warming in late December was not captured by the USMM). 1994 and 1995 show a similar decrease in the projection on PC#1 through most or all of the period, indicating strengthening of the polar vortex; these three years all had unusually strong early-winter polar vortices in the lower stratosphere (e.g. Manney *et al.* 1994b, 1996; Zurek *et al.* 1996). In both 1993 and 1997, there were very strong minor warmings in December (e.g. Manney *et al.* 2001) and this behaviour is reflected in an initial decrease in the time projection on PC#1 with an increase beginning in December. The 1996 early-winter vortex was unusually weak (e.g. Coy *et al.* 1997), and the decrease in PC#1 does not begin until December.

The USMM simulations of the NH early winter show overall very realistic patterns of interannual and intraseasonal variability in the middle and lower stratosphere, even when detailed agreement in synoptic structure between model and analyses is lacking. The model performance is less impressive in the upper stratosphere, but most climatological features are at least qualitatively represented.

5. The southern hemisphere and interhemispheric comparison

Similar USMM simulations were done for 25 April through 4 July in the SH fall/early winter in 1992 through 1997. Figure 14 shows 10 hPa anomaly correlations and biases for SH geopotential heights for each of these simulations. As in the NH, there are substantial variations in the detailed success of the simulations from year to year, but in general the anomaly correlations are high and significant at the 95% level during most of the simulations. Biases, on the other hand, are larger than those in the NH, and the USMM has a high bias in each year (indicating a weaker, warmer polar vortex) with respect to the Met Office analyses. The only drop to very low anomaly correlations for a significant period is in early June 1994, during an unusually strong minor warming similar in character to the NH Canadian warmings. Examination of 10 hPa geopotential heights and waves 1 and 2 indicates that disagreement results partially from phase differences, particularly in wave 2, between USMM and Met Office analyses, and partially from consistently larger wave amplitudes in the model.

Figure 15 shows correlation coefficients and biases between USMM and Met Office fields for the daily 6-year average 10 and 1 hPa geopotential heights from 45°S to the pole. The average fields show very high correlation coefficients, but also large high biases in the USMM geopotential heights, generally increasing with time and altitude. Figure 16 shows 6-year average time series of zonal-mean wind, temperature and wave-1 and wave-2 geopotential height for the SH simulation period, and the USMM–Met Office differences. The zonal-mean winds and temperatures agree well poleward of the jet core (~65°S), but, as in the NH, the dipole pattern of differences indicates a higher-latitude jet maximum in the model; the jet maximum is also slightly weaker in the USMM, and strongest winds are confined to a narrower region, resulting in

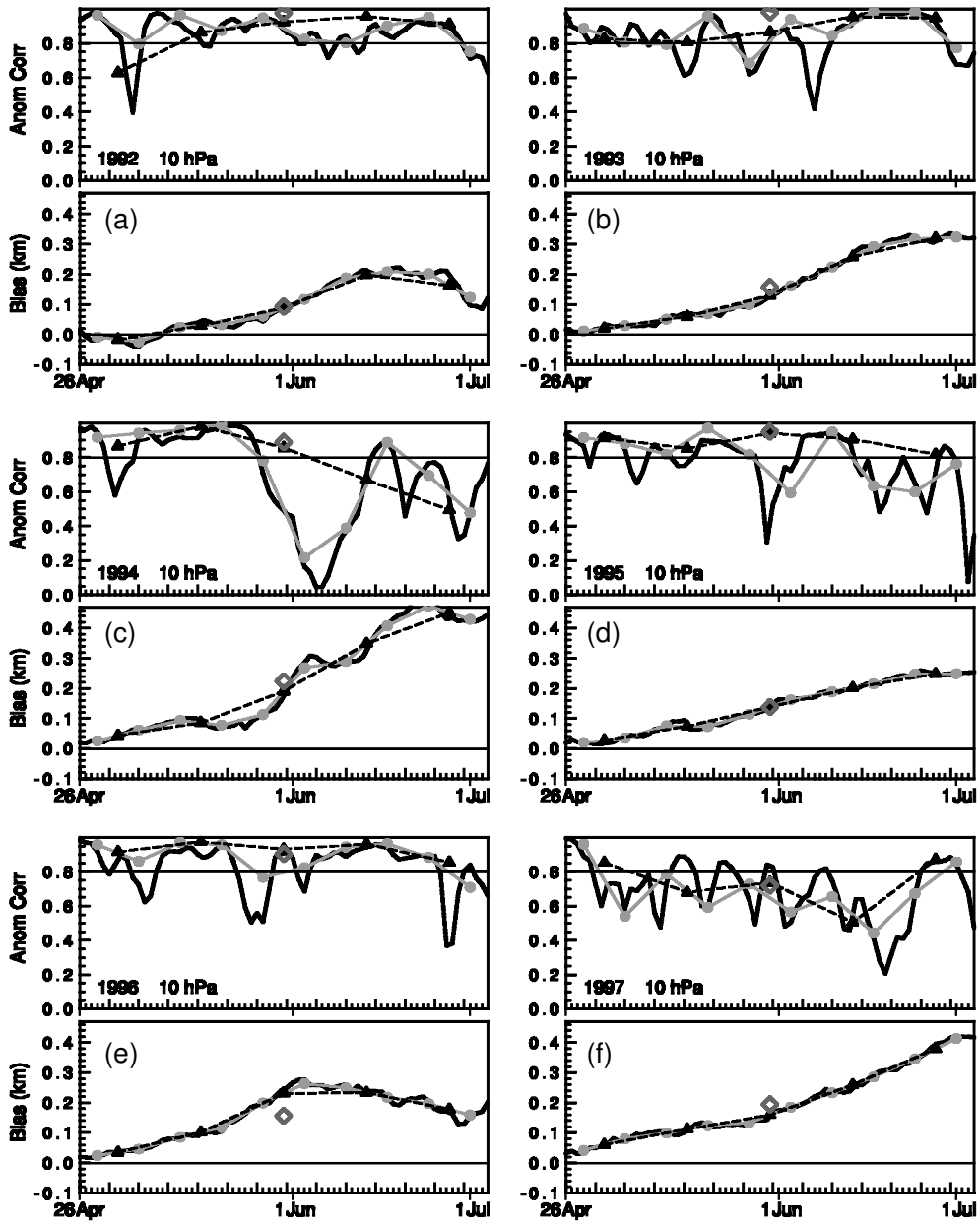

Figure 14. Anomaly correlations (AC, upper panels) and bias (km, lower panels) of 10 hPa Met Office and USMM geopotential heights for the area south of 45°S for simulations of six southern-hemisphere fall/early-winter periods. Thick black lines show correlations and biases on individual days, grey dots and lines for 7-day averages, black triangles and dashed lines for 14-day averages, and large open diamond for the average over the entire 70-day simulation period. The 95% significance level for the correlations is near 0.8 (thin horizontal line in AC panels). Bias is calculated as USMM − Met Office, so negative values indicate lower geopotential heights in the USMM.

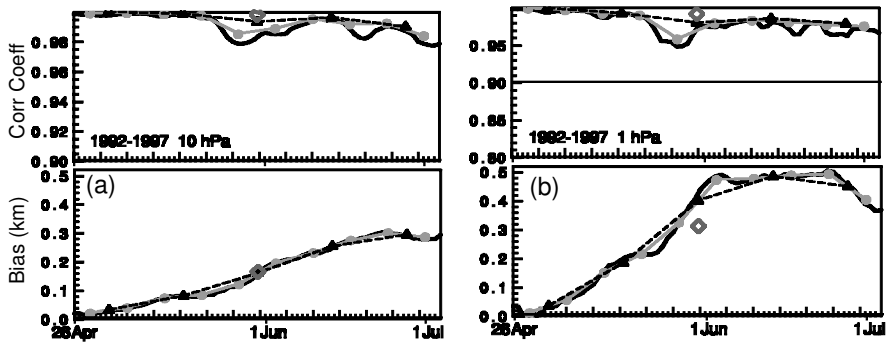

Figure 15. Correlation coefficients (top panels) and bias (bottom panels) between 'climatological' (i.e. 6-year average) Met Office and USMM southern-hemisphere geopotential-height fields at (left) 10 hPa and (right) 1 hPa. Bias is calculated as USMM – Met Office, so negative values indicate lower geopotential heights in the USMM. Layout is as in Fig. 9.

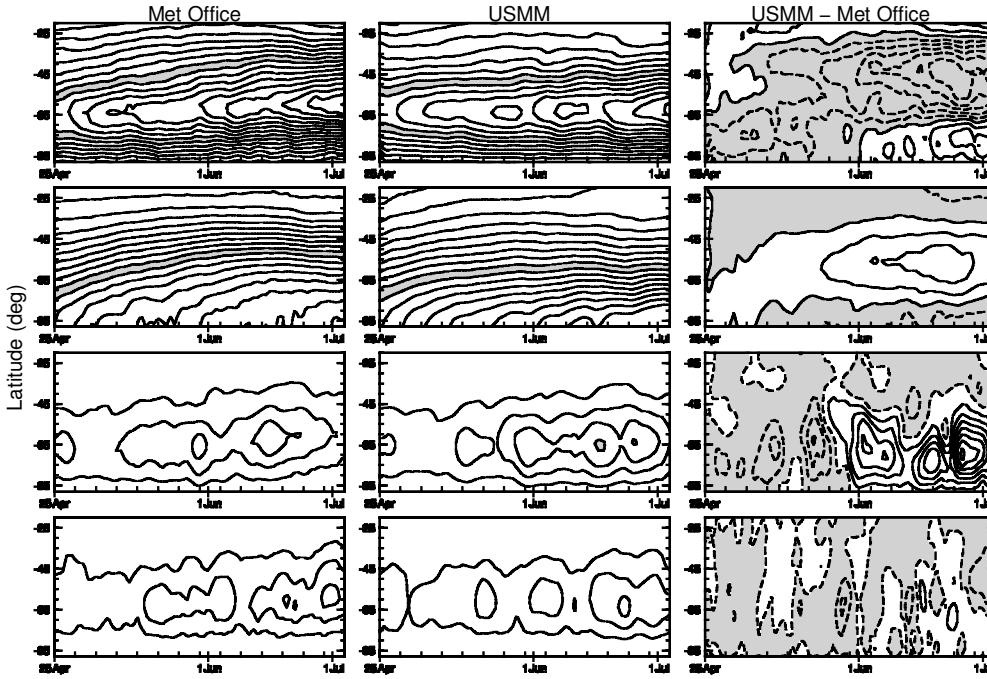

Figure 16. Time series of 6-year average (top to bottom) zonal-mean wind, zonal-mean temperature, geopotential-height wave 1 and geopotential-height wave 2 at 10 hPa in the southern hemisphere, from Met Office (left) and USMM (centre), and the USMM–Met Office difference (right). Contour intervals and shading are as in Fig. 10.

significantly weaker winds and higher temperatures from about 40–60°S in the USMM. As suggested by the bias, the USMM shows larger wave-1 amplitudes in June than does the Met Office analysis. Small decreases in both USMM and Met Office zonal-mean winds in late May to early June suggest a preferred time for early-winter minor warmings in the SH, similar to that seen in the NH.

Rather than the pronounced double peak in the upper-stratospheric jet seen in the NH (Fig. 11), the SH early-winter upper-stratospheric jet (Fig. 17(a) shows 1–5 June)

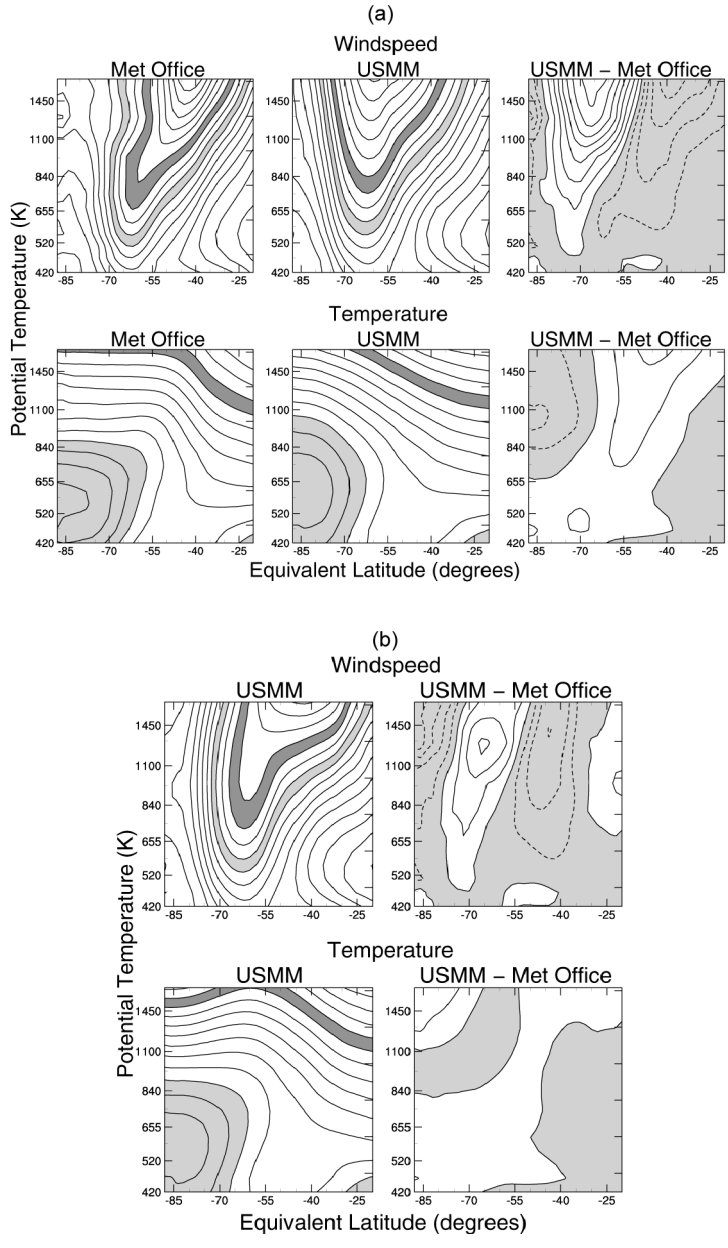

Figure 17. (a) Cross-sections of wind speed (top) and temperature (bottom) as a function of θ and equivalent latitude averaged over 1–5 June and over the 6 years simulated in the southern hemisphere, for Met Office (left), USMM (centre, RF runs, see text) and the difference, USMM − Met Office (right). Contour intervals and shading are as in Fig. 11. (b) Cross-sections of wind speed (top) and temperature (bottom) as a function of θ and equivalent latitude averaged over 1–5 June and over the 6 years simulated in the southern hemisphere, for USMM GW runs (see text, left) and the USMM–Met Office difference (right). Contour intervals and shading are as in Fig. 11.

has a strong equatorward tilt with height, resulting in a very large vortex in the upper stratosphere and a smaller vortex in the lower stratosphere. The failing of the RF USMM runs in the upper stratosphere is, however, similar to that in the NH, in that the model does not reproduce the strong equatorward tilt of the jet. Jet structures agree well only below about 800 K. Met Office and USMM maximum wind speeds are similar throughout the stratosphere—but the shape and position of the jet are not well simulated. As was the case for the NH, this failure is largely related to the Rayleigh friction parametrization of gravity-wave drag. Figure 17(b) shows the same fields as Fig. 17(a) for SH GW USMM runs, which come closer than the RF runs to mimicking the shape of the upper-stratospheric jet seen in the Met Office analyses (although the maximum wind speeds in the upper stratosphere are too weak in the GW runs).

Polar temperatures in the lower stratosphere are only slightly higher in the RF model runs than in the Met Office analyses (Fig. 17(a)). In the middle and upper stratosphere, polar temperatures are lower in the USMM than in the Met Office analyses, but the cold region has larger latitudinal extent in the Met Office analyses in the middle stratosphere. The GW runs reduce these climatological differences in temperature somewhat (Fig. 17(b)), and are slightly warmer than the Met Office analyses in both the upper and lower stratosphere. The overall time evolution of both temperatures and wind speeds is comparable in the model and the analyses. Although the GW runs produce improvements in the structure of the upper-stratospheric jet, this is again at the expense of degradation in the agreement of USMM planetary-wave amplitudes and phases with those in the Met Office analyses.

The time mean, standard deviations, and first three PCs from the SH EOF analysis of 10 hPa geopotential heights are shown in Fig. 18. Striking similarities to the patterns in the NH (Fig. 12) are evident. While the SH time mean is more symmetric than that in the NH, the maximum variability in the standard deviations is again in a crescent shape near 60–80°, located in this case over the South Pacific. This is the region noted by Farrara *et al.* (1992) as the preferred location for the SH early-winter warmings analogous to Canadian warmings. Interestingly, Scaife *et al.* (2000) showed largest interannual variability in July and August in the SH in a similar crescent pattern, but shifted 45–60° west of these early-winter maxima. Examination of standard deviations from averages over the 6 years for periods throughout the runs, and for time averages of individual runs, indicate that in the SH, the positions of both maximum intraseasonal and interannual variability vary with time. The magnitude of the total variability seen in Fig. 18 is only a little less than that seen in the NH. The Met Office fields show stronger variability than either the model or the longer record of NCEP data.

PC#1 in the SH is again an annular mode, and the decrease in the time projections on it to substantial negative values through the simulation periods indicates the strengthening of the polar vortex (Fig. 19 shows 1993). The exact pattern of PC#1 is less similar between the three EOF analyses than the three PC#1 patterns were in the NH, with the longer record of NCEP data showing a more zonally symmetric pattern, and an ~90° phase difference between the Met Office and USMM patterns at high latitudes. PC#2 and PC#3 are very similar to those in the NH, largely wave-1 patterns distinguished by a 90° phase shift. The most striking difference between NH and SH is in the amount of variance explained by PC#1 versus higher PCs. In the observed fields (Met Office and NCEP), PC#1 explains 94–96% of the variance in the SH, as opposed to 71–76% in the NH. While in the NH, the model PC#1 explains about the same amount of variance as in the data, in the SH USMM PC#1 explains only 80% of the variance, with the significant remainder explained by PC#2 and PC#3. This underscores again the overall presence of more wave activity in the SH USMM runs than in the analyses.

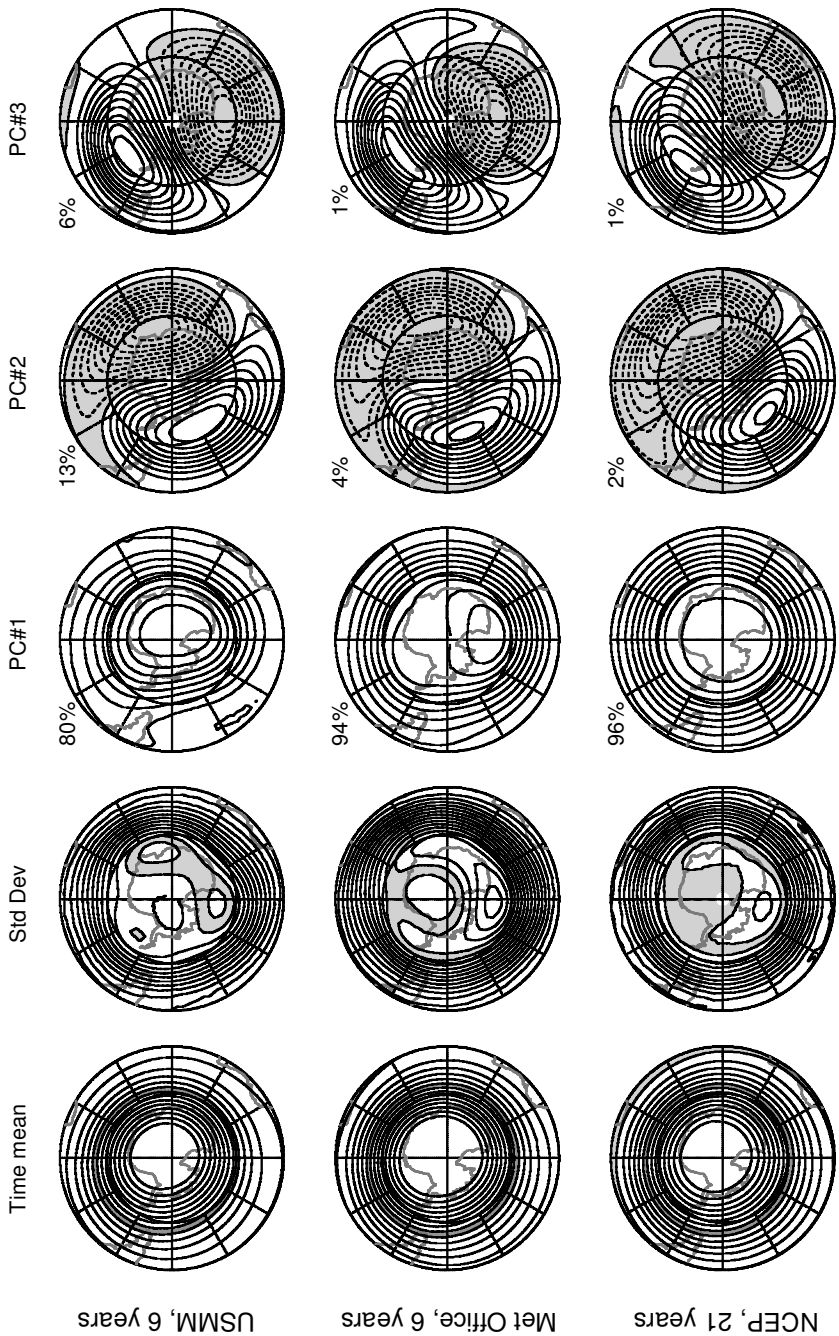

Figure 18. Time mean, standard deviation and first three empirical orthogonal functions of the 10 hPa geopotential heights in the southern hemisphere for 26 April through 4 July from (top) USMM for 6 years, 1992–97; (centre) Met Office for 6 years, 1992–97; and (bottom) NCEP for 21 years, 1979–99. Geopotential-height contour interval is 0.2 km, with 29.8–30 km shaded; standard-deviation contour interval is 0.04 km, with 0.52–0.56 km shaded; principal component (PC) fields are normalized, with contours from −1 to 1 by 0.1 and negative values shaded.

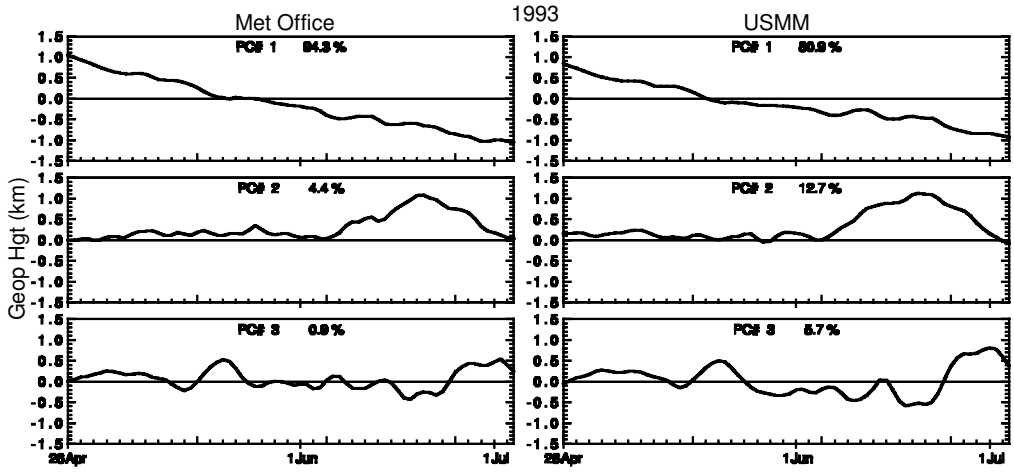

Figure 19. Time projections of 10 hPa geopotential height onto the first three empirical orthogonal functions from (left) Met Office and (right) USMM, for the 1993 southern-hemisphere early winter.

EOFs for the SH GW runs show a similar PC#1 (85%) pattern, and both PC#2 (10%) and PC#3 (4%) shifted westward from the patterns in the RF runs; the maximum in standard deviation is shifted to near 90°E in the GW runs.

The time projections shown in Fig. 19 for 1993 are very similar to those in each of the other years in the SH, the dominant effect being the strengthening of the vortex reflected in the steady decrease in the heights projected on PC#1. Similar patterns are seen for PC#2 and PC#3 from Met Office and USMM, as is the case for the other SH simulations. Correlation coefficients are usually significant at or near the 95% confidence level; for 1993, they are significant at the 99% confidence level for PC#2 and PC#3, and just below the 95% level for PC#1.

6. Discussion and conclusions

We have examined mechanistic model simulations of six early-winter periods in the northern (25 October through 3 January) and southern (25 April through 4 July) hemispheres, to assess the ability of the model to simulate individual early winters and to capture the climatology and variability typical of early winter. Examination of these simulations, and the meteorological data they are compared with, also gives a more comprehensive picture of typical features of the stratospheric circulation during early winter, and interhemispheric differences and similarities in this circulation.

The USMM simulations of the six NH early winters from 1992 through 1997 show detailed success, as indicated by pattern correlations, in reproducing the day-to-day features of stratospheric fields in 3 of the 6 years. Comparison of synoptic fields and their time evolution indicates that, even in the simulations with lower pattern correlations, much of the difference between model and analysis can be attributed to phase differences between USMM and Met Office fields, particularly in the wave-2 phase. Some differences are also seen in the relative wave-1 and wave-2 amplitudes. These results are consistent with those of Mote *et al.* (1998) who found that the model did less well in their simulations in reproducing wave-2 than wave-1 eddies. EP fluxes agree well for the three more successful simulations, and at most times during the less successful ones; disagreements often reflect differences of up to a few days in the time

of wave activity changes. The comparisons of synoptic evolution and wave propagation indicate that, even in the less successful simulations, many characteristics of the day-to-day evolution of the stratospheric flow are simulated well.

The three more successful simulations are for years when there are QBO westerlies in the NH mid- to lower-stratosphere tropics. However, the modelled equatorial winds, EP fluxes, and high-latitude zonal-mean winds do not show any apparent overall pattern to, or even consistently larger differences in the magnitude of, model–analysis differences in years with poor simulations. The differences that result in poor pattern correlations during the easterly QBO periods are mainly in planetary-wave phases, and to a lesser degree, amplitudes. Planetary-wave characteristics and propagation are in turn sensitive—in a complex manner—to subtle differences in the zonal-mean winds throughout the stratosphere and to details of the boundary fields. It is thus extremely difficult to diagnose whether the QBO phase may be affecting the skill of the simulations. Substantial further work would be needed to address this question, including simulation of many more than 6 years to see whether or not the pattern of less model skill during easterly QBO phase holds, possibly including model runs with an imposed QBO.

The model simulates an overall realistic climatology of the NH stratospheric flow in fall/early winter. On average (although this is not true of each individual year), the model produces a slightly stronger jet and lower temperatures throughout the polar stratosphere than those in the Met Office analyses. The model and analyses both indicate a clustering of early-winter minor warmings in late November/early December. Greatest variability is seen in a crescent region near 60–80°N located near the dateline, and is comparable in magnitude in the USMM simulations, the Met Office analyses for the same years, and a longer, 19-year record of NCEP data. The patterns resulting from EOF analyses also are very similar in all three of these records, and show most of the variance (~70–75%) explained by an annular mode, and most of the remainder by two 90°-out-of-phase modes dominated by wave 1. These two modes reflect the dominance of wave 1 during this period, when the Aleutian high is developing, and the anticyclone is often temporarily intensified by predominantly wave-1 minor warmings.

A notable failure in the climatology of the model simulations is that they do not, even in the most successful runs, capture as strong a double-jet pattern in the NH upper stratosphere as is seen in the Met Office analyses. The model does produce a double jet, but the poleward branch is always stronger than the equatorward branch; in contrast, the Met Office analyses for late November and early December often show a stronger equatorward branch. This failure is related to the Rayleigh friction used to parametrize gravity-wave drag; runs using a non-orographic gravity-wave parametrization produce a jet structure in the upper stratosphere that more closely matches that in the analyses.

In the SH, the individual simulations showed strong pattern correlations, with only a few periods below the 95% significance level. In contrast to the NH, the model–analysis bias was consistent from year to year, with a weaker and warmer polar vortex throughout the stratosphere in the model. Examination of synoptic fields shows similar failings underlying periods of poor model–analysis correlation—that is, much of the difference results from phase differences between modelled and observed planetary waves.

The climatology in the SH is also fairly well simulated, although biases between the model and analysis are larger than in the NH. As in the NH, the model is less successful in reproducing the structure of the upper-stratospheric jet. In the SH, the jet broadens at the top and slopes strongly equatorward; the USMM does not capture this strong equatorward tilt, resulting in a narrower and more upright modelled upper-stratospheric jet; this problem is also reduced when the non-orographic gravity-wave parametrization is used.

Similar to the patterns seen in the NH, the largest variability in the SH is in a crescent at 60–80°S centred over the South Pacific, and is comparable in magnitude in the model and the analyses, including that of a 21-year series of NCEP data. The South Pacific is the preferred region for early-winter minor warmings in the SH (e.g. Farrara *et al.* 1992). The dominant modes of the EOF analysis also strongly resemble those in the NH, being a strongly dominant annular mode and two 90°-out-of-phase 'wave 1' modes. The main difference is that in the SH observational analyses, the annular mode explains 90–95% of the variance, as opposed to 70–75% in the NH. The larger model bias in the SH is reflected in the fact that the annular mode explains only about 80% of the variance in the USMM runs, with the more dominant 'wave 1' mode explaining the bulk of the remainder.

While using the non-orographic gravity-wave parametrization rather than Rayleigh friction produces notable improvement in some aspects of the modelled climatology in both hemispheres, particularly in the shape of the upper-stratospheric jet, in most cases it also degrades other aspects of the simulations, especially the planetary-wave phases and amplitudes in the mid-stratosphere. While extensive 'tuning' might allow selection of parameters that produced 'better' overall simulations, and could potentially provide some insight into the sensitivity of planetary-wave characteristics to the inclusion of gravity-wave drag, such tuning is very computationally expensive, and has little solid physical or observational foundation; also, because of expected interannual and interhemispheric variability in gravity-wave activity, no single set of parameters is likely to always be optimal. As pointed out in previous studies, fuller observation-based characterization of the interannual and spatial variability in gravity-wave activity would be an invaluable aid to modelling, especially for mechanistic models such as the USMM where tropospheric mechanisms for gravity-wave generation cannot be explicitly included.

Interhemispheric comparisons show very similar circulation patterns in the NH and SH early winters. Both show a strengthening vortex with wave activity strongly dominated by wave 1. As noted by Farrara *et al.* (1992) both experience minor warmings with characteristics like those of Canadian warmings. Farrara *et al.* (1992) also showed that the SH minor warmings were closely linked to the evolution of wave 1 in the boundary field; consistent with this, USMM runs with higher wave numbers removed from the boundary fields produced fairly good simulations for 1992. This suggests that much of the variability seen in the early-winter stratosphere of both hemispheres is closely linked to the lower-boundary forcing, as opposed to arising primarily from internal variability, as has been seen to be possible in some more idealized studies (e.g. Scott and Haynes 1998; Christiansen 1999, 2000, and references therein). An interesting question for further modelling studies would be to explore the dependence on details of the lower-boundary forcing of the model–analysis planetary-wave phase differences that comprise much of the disagreement.

Early-winter warmings occur preferentially at equivalent times, near the beginning of December (June) in the NH (SH). Both hemispheres show strongest variability during early winter at the location favoured for the formation of an anticyclone during minor warmings. In the NH, the interannual variability shows a maximum near the same location throughout the simulations, while in the SH, the location of maximum interannual variability changes during the period of the simulations. The differences in the broad characteristics of the NH and SH early-winter circulations are mainly quantitative rather than qualitative—in the SH, early-winter warmings are weak, and the vortex is stronger and more symmetric. The qualitative similarity is in contrast to studies of middle and late winter (e.g. Scaife *et al.* 2000, and references therein),

which find substantial qualitative differences between NH and SH circulations. Scaife and James (2000) examined small-, moderate-, and large-amplitude steady wave forcing at the lower boundary in idealized mechanistic model simulations and found a crescent pattern in the resultant interannual variability for small- to moderate-forcing regimes, similar to the patterns shown here in both hemispheres for early winter, and to that shown by Scaife *et al.* (2000) for the SH middle and late winter. Thus it seems that the wave forcing in early winter in the NH may not yet be strong enough to produce a 'strong-forcing' regime (Scaife *et al.* 2000) like that seen in the NH middle to late winter, resulting in the qualitative similarity between the NH and SH stratospheric flow in early winter.

The overall results show some success in simulating many details of the early-winter circulation in both hemispheres, although the degree of this success varies from year to year. One useful result of these simulations is that they reproduce realistic climatology and variability in the early-winter stratosphere. Further analyses of these and additional simulations may be useful in quantifying other characteristics of the evolution of the stratospheric circulation in early winter and the transport associated with it; work is currently in progress analysing the variability in long-lived trace-gas fields from these simulations. Some characteristics of these early-winter simulations, and their sensitivity to model changes, also suggest further studies that could help to quantify mechanisms in the early-winter stratosphere. The relationship of planetary-wave phases, wave propagation, and model skill in these simulations are being explored further using three-dimensional EP fluxes (e.g. Plumb 1985; Sabutis *et al.* 1997). Other studies of interest may include: further simulations with modified lower-boundary fields (time invariant, and/or modified wave amplitudes) to examine the relative role of direct forcing versus internally generated variability, and the influence of the boundary fields on model skill in simulating planetary-wave phases and amplitudes; simulations with an imposed QBO to explore whether the QBO does, indeed, affect the skill of the simulations; and further experiments with non-orographic gravity-wave parametrizations.

ACKNOWLEDGEMENTS

We thank the Met Office (especially Richard Swinbank) and NCEP for meteorological data and advice on their use, John Thuburn for advice on USMM runs and help with the gravity-wave parametrization, and Ian MacKenzie, Phil Mote and Peter Stott for helpful comments or discussions. Research at the Jet Propulsion Laboratory, California Institute of Technology was performed under contract with the National Aeronautics and Space Administration.

REFERENCES

Andrews, D. G., Holton, J. R. and Leovy, C. B. 1987 *Middle Atmosphere Dynamics*. Academic Press, San Diego, CA, USA

Baldwin, M. P. and Holton, J. R. 1988 Climatology of the stratospheric polar vortex and planetary wave breaking. *J. Atmos. Sci.*, **45,** 1123–1142

Baldwin, M. P., Gray, L. J., Dunkerton, T. J., Hamilton, K., Haynes, P. H., Randel, W. J., Holton, J. R., Alexander, M. J., Hirota, I., Horinouchi, T., Jones, D. B. A., Kinnersley, J. S., Marquardt, C., Sato, K. and Takahasi, M. 2001 The quasi-biennial oscillation. *Rev. Geophys.*, **39,** 179–229

Bretherton, C. S., Widmann, M., Dymnikov, V. P., Wallace, J. M. and Bladé, I. 1999 The effective number of spatial degrees of freedom of a time-varying field. *J. Climate*, **12,** 1990–2000

Butchart, N. and Remsberg, E. E. 1986 The area of the stratospheric polar vortex as a diagnostic for tracer transport on an isentropic surface. *J. Atmos. Sci.*, **43,** 1319–1339

Christiansen, B. 1999 Stratospheric vacillations in a general circulation model. *J. Atmos. Sci.*, **56,** 1858–1872

2000 Chaos, quasiperiodicity, interannual variability: Studies of a stratospheric vacillation model. *J. Atmos. Sci.*, **57,** 3161–3173

Clough, S. A., Grahame, N. S. and O'Neill, A. 1985 Potential vorticity in the stratosphere derived using data from satellites. *Q. J. R. Meteorol. Soc.*, **111,** 335–358

Coy, L., Nash, E. R. and Newman, P. A. 1997 Meteorology of the polar vortex: Spring 1997. *Geophys. Res. Lett.*, **24,** 2693–2696

Dequé, M. 1997 Ensemble size for numerical seasonal forecasts. *Tellus*, **49A,** 74–86

Dunkerton, T. J. and Baldwin, M. P. 1991 Quasi-biennial modulation of planetary-wave fluxes in the northern hemisphere winter. *J. Atmos. Sci.*, **48,** 1043–1061

Farrara, J. D., Fisher, M., Mechoso, C. R. and O'Neill, A. 1992 Planetary-scale disturbances in the southern stratosphere during early winter. *J. Atmos. Sci.*, **49,** 1757–1775

Freund, J. E. 1971 *Mathematical Statistics*. Prentice Hall, New Jersey, USA

Gray, L. J. 2000 A model study of the influence of the quasi-biennial oscillation on trace gas distributions in the middle and upper stratosphere. *J. Geophys. Res.*, **105,** 4539–4551

Gray, L. J., Drysdale, E. F., Dunkerton, T. J. and Lawrence, B. N. 2001 Model studies of the interannual variability of the northern-hemisphere stratospheric winter circulation: The role of the quasi-biennial oscillation. *Q. J. R. Meteorol. Soc.*, **127,** 1413–1432

Harvey, V. L. and Hitchman, M. H. 1996 A climatology of the Aleutian high. *J. Atmos. Sci.*, **53,** 2088–2101

Juckes, M. N. and O'Neill, A. 1988 Early winter in the northern hemisphere. *Q. J. R. Meteorol. Soc.*, **114,** 1111–1125

Labitzke, K. 1977 Interannual variability of the winter stratosphere in the northern hemisphere. *Mon. Weather Rev.*, **105,** 762–770

1982 On the interannual variability of the middle stratosphere during the northern winters. *J. Meteorol. Soc. Jpn.*, **60,** 124–139

Lahoz, W. A. 1999 Predictive skill of the UKMO Unified Model in the lower stratosphere. *Q. J. R. Meteorol. Soc.*, **125,** 2205–2238

Lawrence, B. N. 2001 A gravity-wave induced quasi-biennial oscillation in a three-dimensional mechanistic model. *Q. J. R. Meteorol. Soc.*, **127,** 2005–2021

Livezey, R. E. and Chen, W. Y. 1983 Statistical field significance and its determination by Monte Carlo techniques. *Mon. Weather Rev.*, **111,** 46–59

McIntyre, M. E. and Palmer, T. N. 1983 Breaking planetary waves in the stratosphere. *Nature*, **305,** 593–600

1984 The 'surf zone' in the stratosphere. *J. Atmos. Terr. Phys.*, **46,** 825–849

MacKenzie, I. A., Harwood, R. S., Stott, P. A. and Watson, G. C. 1999 Radiative-dynamic effects of the Antarctic ozone hole and chemical feedback. *Q. J. R. Meteorol. Soc.*, **125,** 2171–2203

Manney, G. L. and Sabutis, J. L. 2000 Development of the polar vortex in the 1999–2000 Arctic winter stratosphere. *Geophys. Res. Lett.*, **27,** 2589–2592

Manney, G. L., Farrara, J. D. and Mechoso, C. R. 1994a Simulations of the February 1979 stratospheric sudden warming: Model comparisons and three-dimensional evolution. *Mon. Weather Rev.*, **122,** 1115–1140

Manney, G. L., Zurek, R. W., Gelman, M. E., Miller, A. J. and Nagatani, R. 1994b The anomalous Arctic lower stratospheric polar vortex of 1992–1993. *Geophys. Res. Lett.*, **21,** 2405–2408

Manney, G. L., Zurek, R. W., Lahoz, W. A., Harwood, R. S., Gille, J. C., Kumer, J. B., Mergenthaler, J. L., Roche, A. E., O'Neill, A., Swinbank, R. and Waters, J. W. 1995 Lagrangian transport calculations using UARS data. Part I: Passive tracers. *J. Atmos. Sci.*, **52,** 3049–3068

Manney, G. L., Santee, M. L., Froidevaux, L., Waters, J. W. and Zurek, R. W. 1996 Polar vortex conditions during the 1995–96 Arctic winter: Meteorology and MLS ozone. *Geophys. Res. Lett.*, **23,** 3203–3206

Manney, G. L., Lahoz, W. A., Swinbank, R., O'Neill, A., Connew, P. M. and Zurek, R. W. 1999 Simulation of the December 1998 stratospheric major warming. *Geophys. Res. Lett.*, **26,** 2733–2736

Manney, G. L., Michelsen, H. A., Irion, F. W., Gunson, M. R., Toon, G. C. and Roche, A. E. 2000 Lamination and polar vortex development in fall from ATMOS long-lived trace gases observed during November 1994. *J. Geophys. Res.*, **105,** 29023–29038

Manney, G. L., Sabutis, J. L. and Swinbank, R. 2001 A unique stratospheric warming event in November 2000. *Geophys. Res. Lett.*, **28,** 2629–2632

Miyakoda, J., Hembree, G. D., Strickler, R. F. and Shulman, I. 1972 Cumulative results of extended forecast experiments: 1. Model performance for winter cases. *Mon. Weather Rev.*, **100,** 836–849

Mote, P. W., Stott, P. A. and Harwood, R. S. 1998 Stratospheric flow during two recent winters simulated by a mechanistic model. *Mon. Weather Rev.*, **126,** 1655–1680

Nicholls, N. 2001 The insignificance of significance testing. *Bull. Am. Meteorol. Soc.*, **82,** 981–986

Norton, W. A. and Thuburn, J. 1997 The mesosphere in the extended UGAMP GCM. Pp. 383–401 in *Gravity wave processes and their parameterization in global climate models*. Ed. K. Hamilton. Springer-Verlag, New York, USA

O'Neill, A. and Pope, V. D. 1990 The seasonal evolution of the extra-tropical stratosphere in the southern and northern hemispheres: Systematic changes in potential vorticity and the non-conservative effects of radiation. Pp. 33–54 in *Dynamics, transport and photochemistry in the middle atmosphere of the southern hemisphere*. Ed. A. O'Neill. Kluwer Acad., Norwell, Mass., USA

Palmer, T. N., Shutts, G. J. and Swinbank, R. 1986 Alleviation of a systematic westerly bias in general circulation and numerical weather prediction models through an orographic gravity wave drag parameterization. *Q. J. R. Meteorol. Soc.*, **112,** 1001–1039

Plumb, R. A. 1985 On the three-dimensional propagation of stationary waves. *J. Atmos. Sci.*, **42,** 217–229

Randel, W. J., Wu, F., Swinbank, R., Nash, J. and O'Neill, A. 1999 Global QBO circulation derived from UKMO stratospheric analyses. *J. Atmos. Sci.*, **56,** 457–474

Rind, D., Suozzo, R. and Balachandran, N. K. 1988 The GISS global climate-middle atmosphere model. Part II: Model variability due to interactions between planetary waves, the mean circulations and gravity wave drag. *J. Atmos. Sci.*, **45,** 371–386

Rosier, S. M., Lawrence, B. N., Andrews, D. G. and Taylor, F. W. 1994 Dynamical evolution of the northern stratosphere in early winter 1991/92, as observed by the Improved Stratospheric and Mesospheric Sounder. *J. Atmos. Sci.*, **51,** 2783–2799

Sabutis, J. L. 1997 The short-term transport of zonal mean ozone using a residual mean circulation calculated from observations. *J. Atmos. Sci.*, **54,** 1094–1106

Sabutis, J. L., Turco, R. P. and Kar, S. K. 1997 Wintertime planetary wave propagation in the lower stratosphere and its observed effect on northern hemisphere temperature–ozone correlations. *J. Geophys. Res.*, **102,** 21709–21717

Scaife, A. A. and James, I. N. 2000 Response of the stratosphere to interannual variability of tropospheric planetary waves. *Q. J. R. Meteorol. Soc.*, **126,** 275–297

Scaife, A. A., Austin, J., Butchart, N., Pawson, S., Keil, M., Nash, J. and James, I. N. 2000 Seasonal and interannual variability of the stratosphere diagnosed from UKMO TOVS analyses. *Q. J. R. Meteorol. Soc.*, **126,** 2585–2604

Scott, R. K. and Haynes, P. H. 1998 Internal interannual variability of the extratropical stratospheric circulation: The low-latitude flywheel. *Q. J. R. Meteorol. Soc.*, **124,** 2149–2173

Shine, K. P. 1987 The middle atmosphere in the absence of dynamic heat fluxes. *Q. J. R. Meteorol. Soc.*, **113,** 603–633

Simmons, A. J. 1986 Numerical prediction: Some results from operational forecasting at ECMWF. *Adv. Geophys.*, **29,** 305–338

Swinbank, R. and O'Neill, A. 1994a Quasi-biennial and semi-annual oscillations in equatorial wind fields constructed by data assimilation. *Geophys. Res. Lett.*, **21,** 2099–2102

1994b A stratosphere–troposphere data assimilation system. *Mon. Weather Rev.*, **122,** 686–702

Swinbank, R., Lahoz, W. A., O'Neill, A., Douglas, C. S., Heaps, A. and Podd, D. 1998 Middle atmosphere variability in the UK Meteorological Office Unified Model. *Q. J. R. Meteorol. Soc.*, **124,** 1485–1525

Thuburn, J. and Brugge, R. 1994 'The UGAMP stratosphere mesosphere model'. Internal Rep. No. 34, UGAMP

Waugh, D. W. and Randel, W. J. 1999 Climatology of Arctic and Antarctic polar vortices using elliptical diagnostics. *J. Atmos. Sci.*, **56,** 1594–1613

Zurek, R. W., Manney, G. L., Miller, A. J., Gelman, M. E. and Nagatani, R. M. 1996 Interannual variability of the north polar vortex in the lower stratosphere during the UARS mission. *Geophys. Res. Lett.*, **23,** 289–292